Chapter 2
Polymer Crystallization – Literature review

2.1 Introduction

While it is not possible to cover the subject of polymer crystallization in a review of this size, it is important in light of author's research to review the fundamental features that are essential to the study of polymer crystallization. The topic itself is central to the present research work, which deals in large part with the crystallization behavior of semicrystalline polyimides. This section thus attempts to cover the important topics in polymer crystallization, the understanding of which is directly or indirectly connected to the present research work. It is also important to look at the fundamental Lauritzen-Hoffman polymer crystallization theory, which was derived originally for flexible polymers like polyethylene. The topics covered in this review encompass several concepts that make the essential foundation on which a significant part of the subsequent research investigation rests.

The Lauritzen-Hoffman theory and its conclusions serve more to establish the general framework for explaining several important observations regarding the crystallization behavior of flexible polymers. While the theory is not readily applicable to more rigid chain polymers like PEEK and aromatic polyimides, it has been used many times without sufficient justification for explaining the crystallization behavior of such rigid chain systems[1]. It can only be said that in future, this theory may serve as a good starting point for better explaining the crystallization behavior of rigid chain systems like polyimides.

2.2 Thermodynamics of crystallization and melting

From thermodynamic considerations alone, a crystal is in a lower free energy state than the liquid when the temperature is below the melting point (T_e^∞) for a large crystal of a very high molecular weight polymer. Figure 2.1 shows schematically the changes in the Gibbs free energy of liquid and a crystal with temperature. The necessary (but not sufficient) criterion for any spontaneous phase transformation (for a constant temperature and constant pressure process) is a negative value of ΔG. Hence the process of crystal formation is spontaneous below the equilibrium melting point(T_m^∞)[**] while the reverse process, i.e. crystal melting to form liquid is spontaneous above T_m^∞. At T_m^∞, a condition of equilibrium exists between the crystal and liquid as both phases have the same value of G and $\Delta G = 0$.

For the case of constant temperature process such as fusion at T_m^∞, $\Delta G_f = 0$ and

$$\Delta G = \Delta H - T\Delta S = 0 \text{ at } T = T_m^\infty \qquad \{2.1\}$$

Thus:

$$T_m^{\ \infty} = \frac{\Delta H_f}{\Delta S_f} = \frac{H_l - H_{cr}}{S_l - S_{cr}} \qquad \{2.2\}$$

Thus both enthalpic and entropic effects will determine the equilibrium melting point for any polymer crystal. While a higher value of ΔH_f leads to a higher T_m^∞, the entropic effects cannot be ignored and are often dominant in deciding the value of T_m^∞. Table 2.1[2] lists the values of T_m , ΔH_f and ΔS_f for a series of polymers and illustrates the effect of

---

[**] While T_e^∞ represents the melting point of an infinitely long crystal of an infinite molecular weight polymer, T_m^∞ represents the melting point of an infinitely long crystal of finite molecular weight. In the case M→∞, $T_m^\infty \to T_e^\infty$.
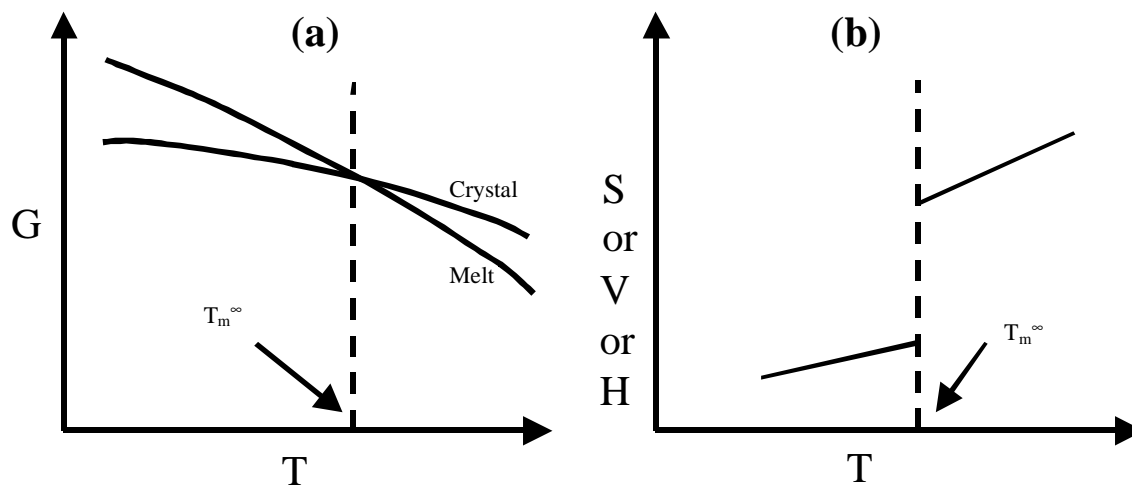
Figure 2.1 General behavior of thermodynamic variables at the equilibrium melting temperature T_m^∞ (a) gibbs free energy (b) entropy and volume.

Table 2.1   Values of T_m, ΔH_f and ΔS_f for various polymers[2].

Polymer	T_m (°C)	ΔH_f (J/mol)	ΔS_f (J/(K.mol))
Polyethylene	137.5	4,020	9.8
Poly(1,4-cis-isoprene)	28	4,390	14.5
Poly(decamethylene sebacate	80	50,200	142.3
Poly(decamethylene azetate)	69	41,840	121.3
Poly(decamethylene sebacamide)	216	34,700	71.1
Poly(decamethylene Azelamide)	214	36,800	75.3

varying ΔH_f and ΔS_f. In this regard, it is especially important to visualize the importance of the term 'S_l', the entropy of the liquid state. As shown in the table, while the values of ΔH_f are lesser for the polyamides, the melting points are higher due to lower ΔS_f. This lower value of ΔS_f is in part due to lower value of entropy (S_l) for the amide in the liquid state. The value of S_l is lower due to presence of hydrogen bonding and increased chain stiffness. Similar effects of lower 'S_l' and hence lower ΔS_f could also be important for the class of high melting semicrystalline polyimides, the topic of this proposal. Although comprehensive calculations of these fundamental thermodynamic parameters for semicrystalline polyimides is still lacking in literature, it is widely known (as discussed in Chapter 1) that strong intermolecular forces due to CTC formation exist in polyimides. The inherent stiffness of the chain also contributes to a lower value of 'S_l'.

Gibbs free energy change for a particular phase is expressed as

$$dG = V\ dP - S\ dT \qquad\qquad \{2.3\}$$

where V and S are the volume and entropy of the phase respectively. Taking the partial derivatives of 'G' with respect to P & T in the above equation, we obtain:

$$(\partial G/\partial T)_p = -S \qquad \& \qquad (\partial G/\partial P)_T = V \qquad\qquad \{2.4\}$$

Figure 2.1(b) shows the idealized response of these variables as a function of temperature and at the transition temperature T_m^∞. These first derivatives of 'G' show a step change at the transition temperature T_m^∞ and the transition is called a first-order transition. While the above discussion addresses purely thermodynamic considerations, the kinetic issues do not favor formation of an infinitely large crystal in polymers, which are characterized, by the formation of finite sized crystals. The exact nature and morphology of these crystals however, has been one of the most heavily debated topics in polymer science.

2.3   Crystallization in polymers: structure, models & relationships

The crystallization of polymers can be broadly classified under three groups:
(A) Crystallization during polymerization (B) Crystallization induced by orientation and (C) Crystallization under quiescent condition. While this discussion will only briefly

address type (A) and (B), the last category (C), will be covered in greater detail as it is more pertinent to the present discussion.

(A) Crystallization during polymerization

A special attribute of this kind of polymerization is the formation of macroscopic single polymer crystals[3] (see Figure 2.2 (b)). During such a process the monomers forming a crystal can be joined up into chains by solid state polymerization, while the original "monomer" crystals are preserved. The final polymer crystal is obtained due to chemical reactions at the gas/solid or liquid/solid interface and not just as a consequence of change in physical state of the material as is observed in normal crystallization processes[4]. The final properties of crystals formed by such methods can be very interesting, for e.g. poly (sulfur nitride) crystals formed by such methods conduct electricity like metals along the crystal axis (corresponding to the chain direction) and can even become superconducting at sufficiently low temperatures[5]. The mechanism of such a process can be (a) the simultaneous polymerization and crystallization and (b) successive polymerization and crystallization[5] (see Figure 2.2 (a)). In (a) the primary and secondary bonds are set at the same time, and in (b) the polymerization and crystallization sites can be separated and thus the nature of the polymer segments as yet uncrystallized becomes important[5]. While macromolecular crystallization can occur from only the melt or solution state, the crystallization during polymerization can occur from the monomer being in either gaseous or condensed state. It is thus also possible to get chain folded crystals below the glass transition temperature of the final polymer (e.g. 100°C below T_g for poly (p-xylylenes)[2]).
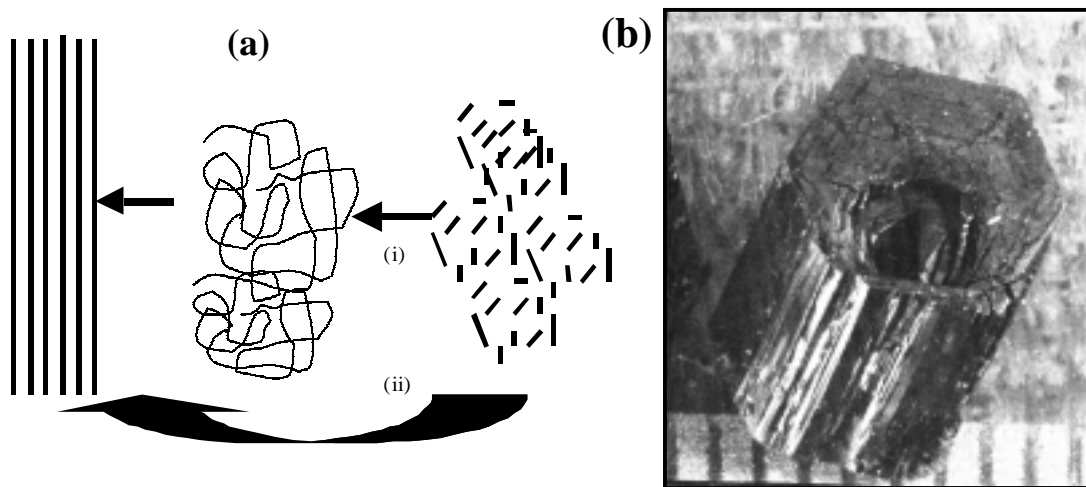
Figure 2.2   (a) Crystallization of macromolecules (i) polymerization followed by crystallization [(i.e.) separate polymerization and crystallization] (ii) crystallization during polymerization[4] and (b) example of macroscopic single crystal obtained by simultaneous polymerization and crystallization-poly (sulfur nitride) 1 division = 0.5 mm (stejny et al.[3])

(B) Crystallization induced by orientation

The schematic of orientation induced crystallization is illustrated in Figure 2.3. The process can be described as stretching of long chains to form fibrous crystals. In fact this is the underlying process governing the formation of fibers though any perfectly smooth and completely elongated chain morphology as illustrated in the schematic is difficult to attain under the most perfect of circumstances. During stretching, the distortion of chains from their most probable conformation results and hence a decrease in the conformational entropy takes place. If this deformation is maintained in this lower conformational entropy state then less conformational entropy needs to be sacrificed by transforming to a crystalline state. This decrease in total entropy of fusion allows the crystallization to occur at higher temperatures than will take place under quiescent conditions. Natural rubber and polyisobutylene are excellent examples of such an effect as they show great propensity to crystallize under stretched conditions whereas they crystallize slowly under quiescent conditions[2]. Also, crystallization in an already oriented polymer results in reduction retractive force[2] (with respect to oriented state). This can be explained on the basis of rubbery elasticity theory according to which the force exerted by fixed chain ends is inversely proportional to number of statistical elements and the magnitude of end to end distance. The reduction in force results, due to lesser number of statistical units available in the amorphous regions and also because the end to end distance of the amorphous units is smaller than the end to end distance in the crystal. Melting of such elongated crystals lead to contraction and crystallization leads to elongation. Thus macroscopic dimensional changes and changes in retractive force can be related to the crystal-liquid phase transformation[2].

Normally, the formation of such fibrous morphology is accompanied by formation of an epitaxial layer over[6] and around the inner fiber giving rise to the so-called 'shish-kebab' kind of morphology[7]. It is well documented[8,9,11] that the outside 'kebab' like regions are essentially folded chain regions comprised of chains which did not crystallize during the orientation process. Thus, while the inner 'shish' regions form first, the formation of folded chain discs occurs due to nucleation events taking place on

the extended chain surface. It is interesting that though the nature of the nucleating surface is a partially extended chain, and thus a great propensity to crystallize into the thermodynamically more favorable extended chain form exists, subsequent crystallization is still of the folded chain type. This has been used as a strong argument in favor of kinetic theories that argue for the chain folded model of crystallization[10]. The lamellar kebabs are usually spaced at distances of ca. 200 to 1000 Å along the chain extended shish. Some researchers have studied the rate of growth perpendicular to the stretch direction and found it to be independent of the percentage extension[11,12,13](though the rate of extension was not a factor in these studies). The unaligned chains, which give rise to this undetachable plate like growth, can be the uncrystallized part of the main chain or totally separate chains. Some researchers found that the central shish was of higher molecular weight than the kebabs, while some[14] have demonstrated that a minimum chain length was required for the chain extension process. It has also been argued that the growth of chain folded structures is aided in large part due to the dangling cilia which mostly result along the central fiber like morphology. These cilia, it has been proposed[10], then act as nucleation sites for the chain folded region to develop.
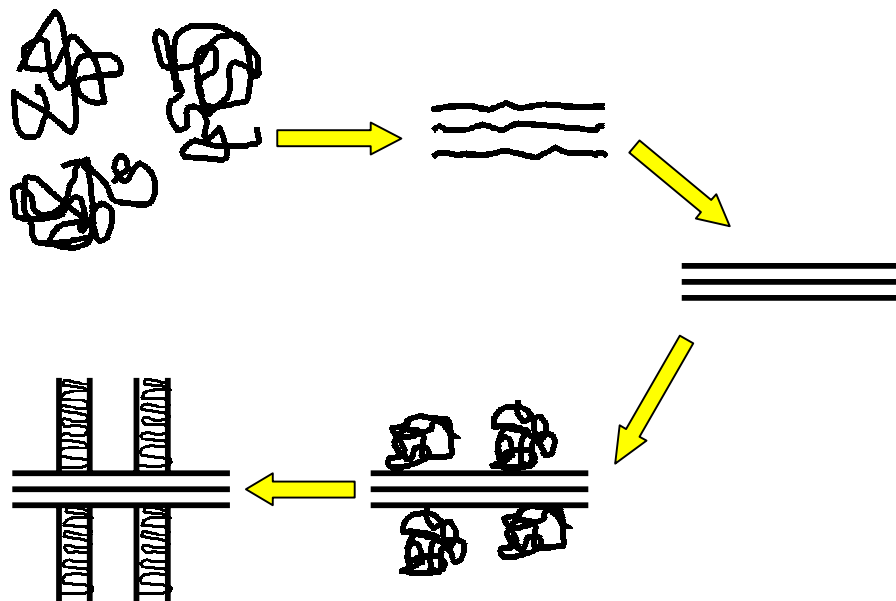
Figure 2.3   Schematic representation of orientation induced crystallization. The first three drawings illustrate the orientation and crystallization of random coils while the last two drawings show the growth of folded chain kebabs around the central shish[10].
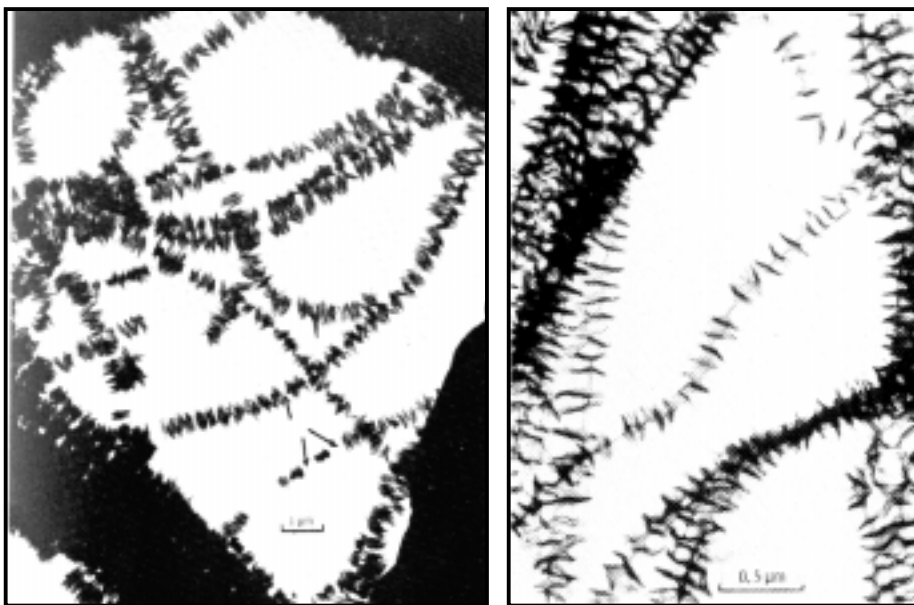

Figure 2.4   (a) Shish kebab morphology of polyethylene from solution (from Pennings, 1967[3]. (b) Shish kebabs of cellulose formed by recrystallizing cellulose II onto microfibrils of high molecular weight[3].

(C) Crystallization under quiescent condition

Crystallization of long-chain flexible molecules of sufficient structural regularity is widely observed under quiescent conditions for a large number of macromolecules of both synthetic and natural origin.   While it has been long established that similar to low molecular weight compounds, polymers can exhibit considerable long range order in the crystalline regions, the exact nature and morphological form of these crystalline regions (specifically at the molecular level) has been a matter of considerable debate.   In this regard it is important to classify the quiescent polymer crystallization into two general types, (1) Crystallization from dilute solutions and (2) Crystallization from the melt. Crystallization from dilute solutions often provides a more fundamental avenue for structural analysis of polymer crystals as these entities can be isolated and precisely studied. Crystallization from the melt is often closer to pragmatic use of the polymer of interest though it adds an additional degree of difficulty to the fundamental structural studies.   While this discussion will refer to results and attributes of dilute solution crystallization intermittently, it is crystallization from the melt that is of direct relevance to the present study.   The nucleation, growth and kinetics of development of these crystalline regions are of both profound fundamental and practical interest. These characteristics are however directly linked to understanding of the morphological detail of these crystalline regions. On this account, there have been various models proposed over the past five decades- each involving considerable amount of controversy and debate, much of that debate persisting even to date. These models are elucidated below, some of which will be elaborated in more detail in the ensuing discussion. The type of morphology can, however, be first classified into two broad classes[10] (1) the fringed micelle model and (2) lamellar type of morphology. The models of lamellar morphology themselves differ on the basis of the nature of the fold surface, type of reentry of the chains and on accounts of presence of an intermediate region for the chain traveling from the crystal to the amorphous phase.

2.4 The fringed micelle model

Hermann, Gerngross and Abitz[15] first conceived this model in 1930 to explain the structure of gelatin, while the model was later more fully expanded by Flory[16,17,18]. The fringed micelle model is based on the idea that parts of the polymer segments (either in solution or in the melt) align themselves together to form bundled crystalline regions (Figure 2.5). These bundles can then grow in the direction of chain axis by reeling in adjoining chain segments (of the chains already part of the crystal) into the crystalline region. Lateral growth of these crystalline regions can also take place by accretion of chain segments from other molecules. The growth of these structures however is
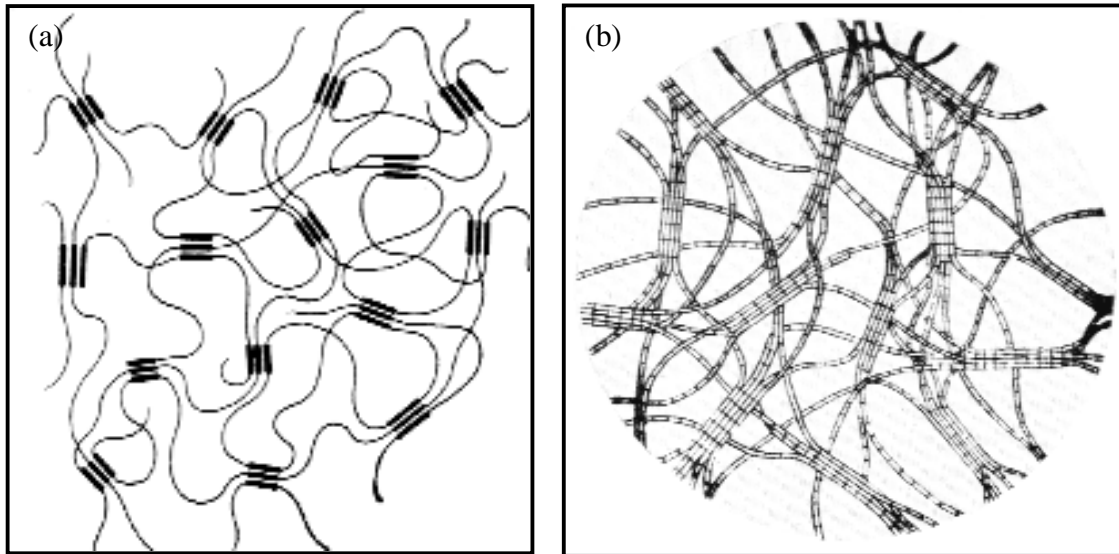
Figure 2.5 Fringed micelle model (a) Model of crystallization as might be visualized in a thermoreversible gel (Keller et al[10].) (b) Hermann and Gerngross model[15] for a semicrystalline polymer. Similar schematics illustrate the general molecular picture in fringed micellar crystallization.

impeded by the presence of entanglements and strained regions, which then constitute the amorphous phase. The "fringes" are the regions of the chains traveling from the crystalline region to the surrounding amorphous regions. The crystalline regions than serve as physical crosslinks.

Some of the first blows to this model of crystallization occurred after collecting evidence of large crystalline superstructures present in such materials, called 'spherulites'. Such a model could not readily explain the growth of such generally spherically symmetrical structures[19]. Also, the birefringence measurements on these spherulites by light microscopy suggested that, for most systems, the polymer chains were more or less tangential in this spherical structure. Although several models were put forward to explain the spherulitic behavior based on this concept[20], they were subsequently abandoned in favor of folded chain lamellar models.

While the fringed model has now long been believed to be inaccurate for describing the common quiescent crystallization behavior, its modifications can still be utilized to explain several phenomena occurring in the crystallization of polymers. Several aspects involving the crystallization of thermoreversible gels - where the dilute solution crystallization leads to 'gelation' of the overall system have been explained on the basis of this model[10,21,22]. Lamellar crystallization, it has been debated, would have lead to the presence of individual single crystals or aggregates thereof. This model has also been widely proclaimed to be correct for certain polymers that crystallize during rapid cooling/quenching from the melt, and where the individual spherulitic detail is not discernible from microscopy[10]. The use of such a model for describing crystallization of an amorphous polymer just above the T_g has been advocated on the grounds of low thermal energy available to chains at such temperatures[19]. At temperatures significantly higher than T_g, these structures will not be stable and will give way to lower energy lamellar form. Additionally the model is utilized to explain the behavior of highly oriented samples like the drawn fibers.

2.5 Lamellar models:

It is a well-established and proven fact that a lamellar crystal is the fundamental structural form by which polymers most generally crystallize, a feature true for the vast majority of semicrystalline polymers crystallized from the bulk (i.e. from solution or from melt). The first report giving evidence of lamellar structures was by Storcks[23] in 1938. He reported electron diffraction results on cast films of gutta-percha and concluded that the films contained microscopic crystals with the molecular axis less than 4° from normal to the plane of the film. He observed that while the electron diffraction results gave only {hk0} reflections, the total length of the chains was much greater than the thickness of the films- a recognition that led him to first propose a chain-folded structure to explain the crystallization in such systems. Schlesinger and Leeper[24] conducted similar experiments in 1953 on gutta-percha but this time using light microscopy and refractive index measurements. While both these studies were largely
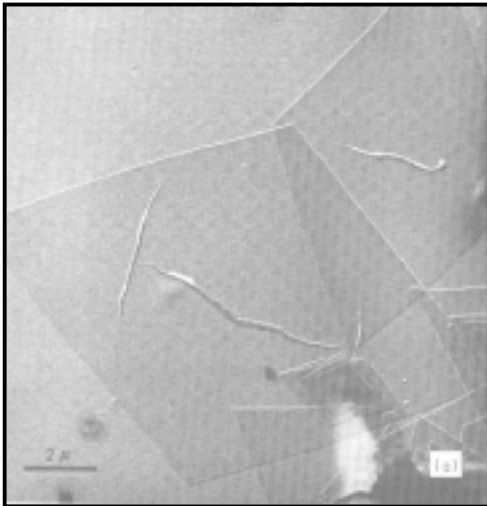
Figure 2.6 Single crystals of Polyethylene after evaporation of tetrachloroethylene solvent. Pleats form due to crystal collapse. Micrograph is taken from 'Polymer Single Crystals' by P.H. Geil[19].

ignored, Jaccodine's report[25] of single crystals of polyethylene in 1955 gained attention of several researchers who expanded on his work. In 1957, Till[26], Keller[27], and Fischer[28] independently reported on the growth and identification of single crystals of polyethylene. Since these studies, lamellar crystal habit has been shown to be the dominant structural mode of crystallization for a large number of polymers. The various models proposed for the nature of these structures are:

(1) Random reentry or "Switchboard" folded model.

This model was first proposed by Flory[17,29,30,31] and consists of chains randomly folding back into the same lamella or even participating in adjoining lamellae. The upper and lower surfaces consist of loops of varying sizes and the amount of adjacent reentry is *small* and *not a necessity*[17,29,30,31]. The upper and lower surfaces may consist of transitional regions that constitute a diffuse phase boundary – their density being intermediate between the crystal and purely amorphous regions.
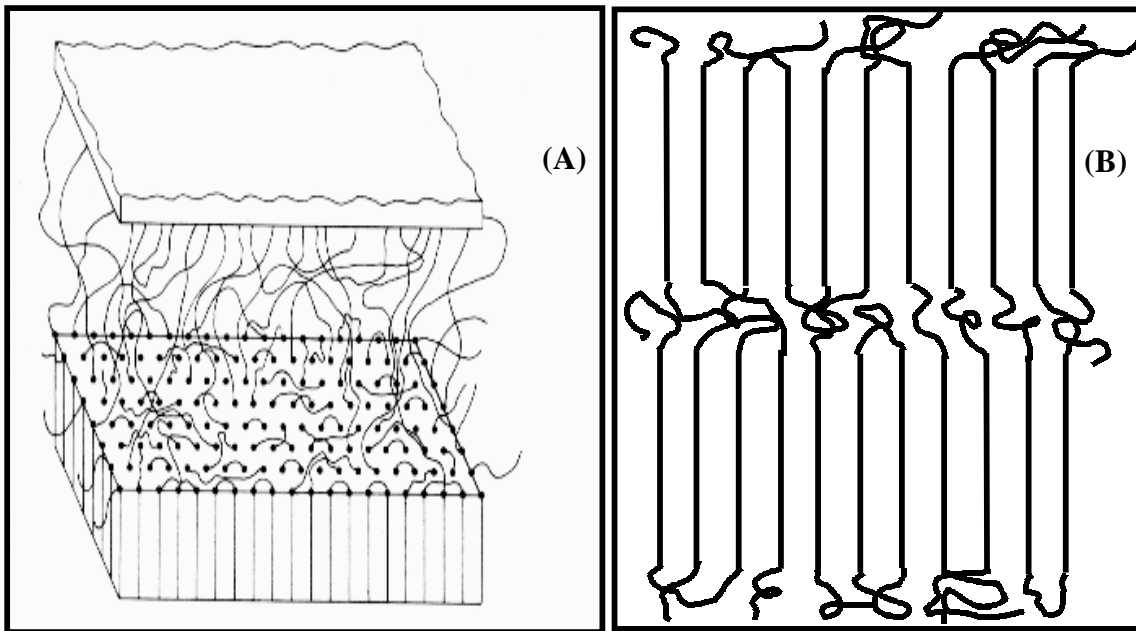

Figure 2.7 (A) Schematic of a Switchboard model, showing the surface of a lamella, interlamellar region and tie chains between the lamella. (From Mandelkern[30]) (B) originally proposed model for melt crystallization in polymers[17].

(2) **Adjacent reentry chain-folded models (regular folding)**

(i)   *Smooth surface model[32,33]:*

This model is characterized by sharp phase boundary between the crystal and the amorphous phase. The mode of reentry of the chains is the adjacent neighbor with only a few exceptions due to multiple nucleation and chain-end defects. This is a very idealized visualization of the chain folding process.

smooth chain-folded surface
(sharp phase boundary)
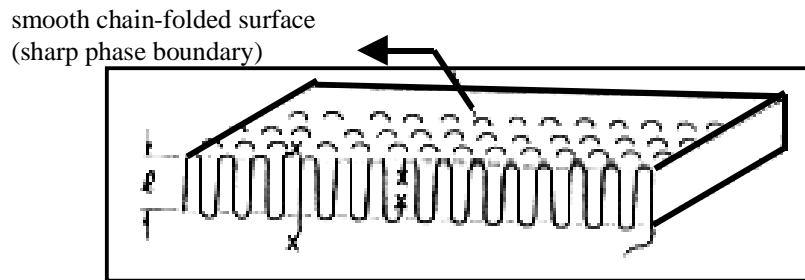
(ii)   *Rough surface model[33]:*

The reentry of the chain is still in the nearest growth plane, though large variations in the fold length may exist on a local scale. Multiple nucleation and chain-end defects will further contribute to a rough surface. The overall phase boundary is no longer sharp, though local regions may still exhibit such character.

rough chain-folded surface

multiple nucleation of molecule
on the growth surface
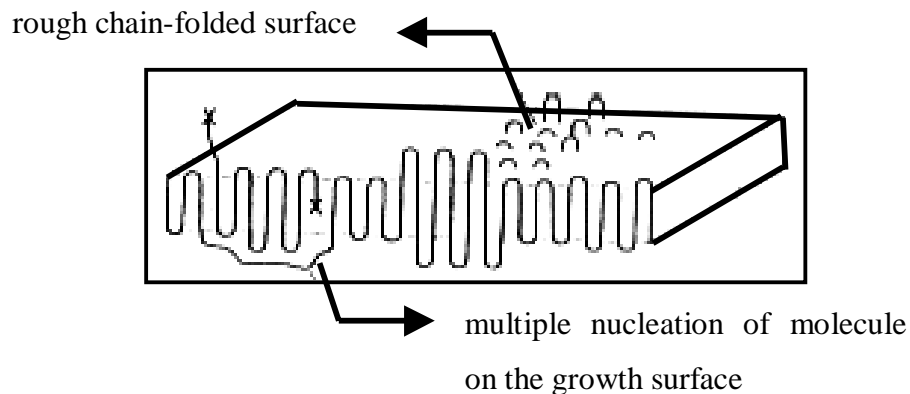
(3)   *"Erstarrungsmodell"* (solidification model)[34,35]

This model was put forward by Fischer & coworkers to explain the constancy of the radius of gyration r_g in the crystalline state (with respect to r_g in the amorphous

state), as detected by small angle neutron scattering (SANS)[36]. The model is similar in conception to the "fringed micellar" morphology and is visualized in terms of alignment of chains without a long-range diffusion process to give rise to a lamellar morphology. The chain sequences in proper conformations (indicated by thicker lines in the diagram) are incorporated into the crystal without significant reorganization of the chain conformation.
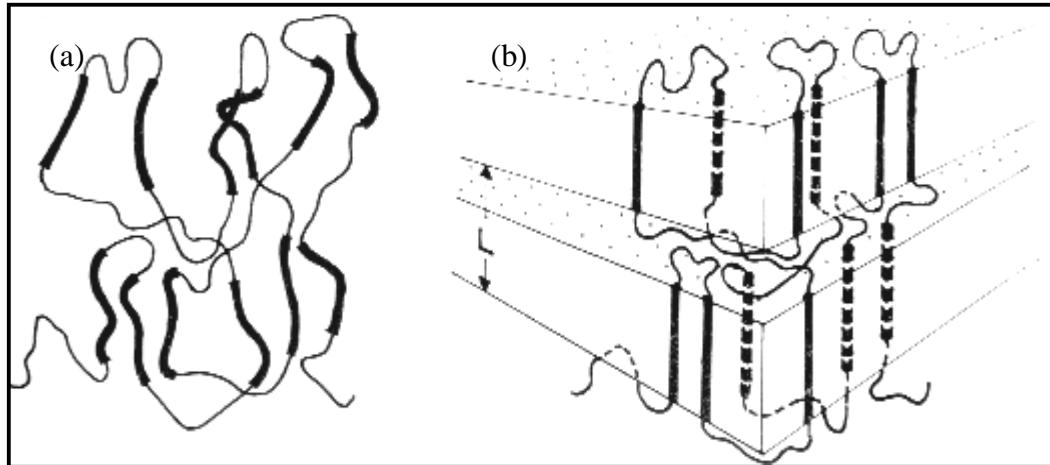
Figure 2.8   "Erstarrungsmodell" (a) chain conformation in the melt state
(b) alignment of suitable conformations in to the crystal[36].

2.6 *Gibbs-Thomson equation*[37,38] *:*

This well known equation is a simple application of fundamental thermodynamic concepts applied to the above discussed lamellar crystal morphology. The existence of a thin plate lamellae with the thickness much smaller than the lateral dimensions is the primary requirement and not the proof of any particular model thereof. The schematic of a lamellar structure, which is shown in figure below, is thus for the purposes of illustration only and the molecular detail should not be taken literally.
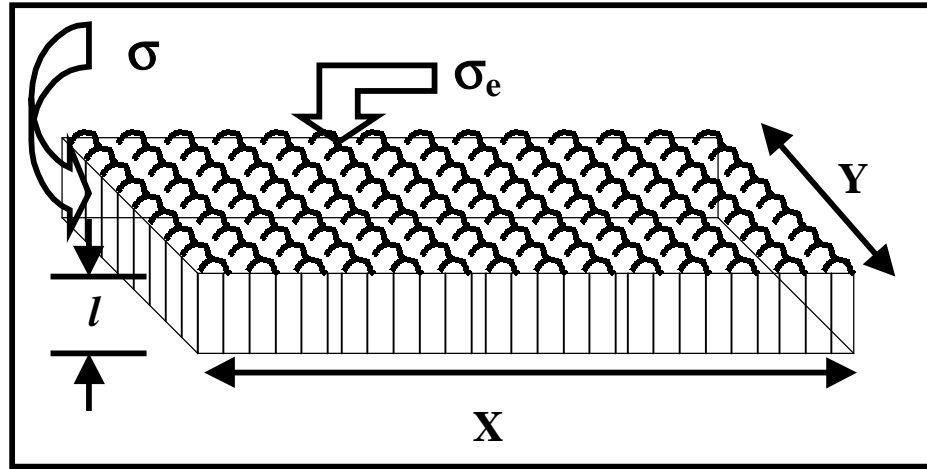
For a finite sized crystal as shown above,

$$\Delta G_{crystal}(T) = 2XY\sigma_e + 2l[X+Y]\,\sigma - XYl\,\Delta G_f^{\infty}\,(T) \qquad \{2.5\}$$

At the melting point of the crystal, T_m:

$$\Delta G_{crystal}(T_m) = 0 \qquad \{2.6\}$$

Assuming:

- 'no thickening'

  - $XY \gg l[X+Y]$ {true for thin lamellae with large lateral dimensions}

  - $\sigma_e \gg \sigma$ {true for most polymers}

  - $X \sim Y$ {does not make a difference for large lateral dimensions}

Eq. (2.5) becomes $\qquad \Delta G_f^{\infty}(T_m) = 2\sigma_e/l \qquad \{2.7\}$

Now for an infinite sized crystal at T_m°,

$$\Delta G_f^{\infty}(T_m^{\circ}) = \Delta H_f^{\infty}(T_m^{\circ}) - T_m^{\circ}\,\Delta S_f^{\infty}(T_m^{\circ}) = 0 \qquad \{2.8\}$$

Hence, $\qquad \Delta S_f^{\infty}(T_m^{\circ}) = \Delta H_f^{\infty}(T_m^{\circ}) / T_m^{\circ} \qquad \{2.9\}$

Now for an infinite sized crystal at T_m,

$$\Delta G_f^{\infty}(T_m) = \Delta H_f^{\infty}(T_m) - T_m\,\Delta S_f^{\infty}(T_m) \neq 0 \qquad \{2.10\}$$

Assuming * $\qquad \Delta H_f^{\infty}(T_m) = \Delta H_f^{\infty}(T_m^{\circ})$ {small temperature dependence is ignored}

$* \quad \Delta S_f^\infty(T_m) = \Delta S_f^\infty(T_m^\circ)$ {not a bad assumption for high T_m's ! }

it is obtained that,

$$\Delta G_f^\infty(T_m) = \Delta H_f^\infty(T_m^\circ) - T_m \Delta S_f^\infty(T_m^\circ) \qquad \{2.11\}$$

using eq.(2.9) $\quad \Delta G_f^\infty(T_m) = \Delta H_f^\infty(T_m^\circ) [1-T_m/T_m^\circ]$ (important relation) {2.12}

comparing eq. (2.7) & eq.(2.12)

$$2\sigma_e/l = \Delta H_f^\infty(T_m^\circ) [1-T_m/T_m^\circ] \qquad \{2.13\}$$

which can be written to give the *Gibbs-Thomson equation*:

$$\boxed{T_m = T_m^\circ \left[1 - \frac{2\sigma_e}{l\Delta H_f^\infty T_m^\circ} \right]} \qquad \{2.14\}$$

This equation provides one of the convenient ways for estimating the value of the equilibrium melting point T_m°, and for also obtaining the value of σ_e. Both these quantities are obtained by plotting the observed melting points T_m vs. $1/l$, where the value of σ_e can be learned from the slope and the intercept gives the value of T_m°. The lamellar thickness 'l' can often be obtained by techniques like SAXS or sometimes TEM whereas T_m is usually obtained using DSC. Many workers[39,40,41] have elucidated the necessary precautions in this method, some of which are:

- lateral dimensions should be $\gg$ thickness of lamellae
- The melting temperature T_m should correspond to the 'l', which, however, is usually measured at room temperature[42] (cause of error for polymers that undergo thickening)[42].

2.7 Lauritzen-Hoffman secondary nucleation theory[43,39]

This theory explains the kinetics of crystallization in molecular terms, for linear flexible macromolecules which are crystallized from the melt into chain folded lamellae. This theory[43] (and its various modifications[32,33,39,44-47]) constitutes perhaps the most comprehensive and widely used methodology to interpret and model the crystallization behavior of a large number of polymers. The theory has evolved substantially since it was first proposed and has incorporated several new concepts in order to broaden the

scope of its predictions and also to satiate the objections of other workers in the field[39]. Though the theory is best suited to describe the chain folded crystallization of polyethylene and other flexible polymers, it has also been applied with some degree of success to model the crystallization behavior of other more rigid chain systems such as PEEK[48]. While it is not possible to fully cover this theory in the present review, the fundamental formalisms and the important deductions will hopefully be succinctly explained in the forthcoming sections.

The original L-H theory and its various modifications account for a broad range of behavior observed for crystallization of linear flexible macromolecules. These are[39]:

- it accounts for the variation of initial lamellar thickness (l^*) vs. supercooling (ΔT_c)

- parameters can be found that fit the variation of crystal growth rate 'G' vs. ΔT_c

- provides an explanation for break in temperature dependence of G

- explains the origin of σ and σ_e

- the generation and effect of adjacent events (tight folding) and non-adjacent events (e.g. tie chains, loose folds, cilia)

- Variation of (a) the crystal growth rate 'G' and (b) quantified chain folding (i.e. degree of tight chain folding), with the change in molecular weight

- Recent versions have also incorporated the 'reptation' concept into the theory

The various facets of polymer crystallization still not addressed completely by the theory are:

- Explanation for primary nucleation and hence bulk crystallization kinetics

- Development of lamellae from a primary nucleus

- Lamellar branching giving rise to spherulites (other factors like screw dislocations provide some explanation)

- Banding in spherulites due to lamellar twisting

- Quantified estimation of the degree of crystallinity

The treatment starts by first addressing the deposition of a first stem and later treating the deposition of subsequent stems in a stepwise manner. The deposition of the stems is

visualized to take place in two steps. In the first step the part of the chain in proximity to the surface loses conformational entropy and becomes flattened with few crystallographic attachments to the surface. The state of the molecule is visualized as being similar to a weak physically adsorbed system with the possibility of occasional point contacts on the surface. This short section of the molecule, after a series of events, straightens and aligns itself to yield an activated state $\Delta\Phi^*$, where the loss in entropy is equal to $\Delta S_f/C_\infty$ (= - ΔS_1^*). The entropic contribution to the free energy barrier will thus be $T\Delta S_f/C_\infty$ with little/no contribution from the heat of fusion at this stage. The second important aspect of first stem deposition is the creation of two new lateral surfaces with work of building them being equal to $2b_0\sigma l$, where b_0 is the layer thickness while 'l' is the length of the chain attached. The value of 'l' is treated as a variable here and later shown to average out to l_g^*. It is these series of steps to yield an activated state, which are considered to be most difficult and slowest. Subsequent stem deposition from this activated state, with the average length of the stem being l_g^*, takes place without any difficulty. According to this, the free energies for the segment of the chain at various states can be written as:

$$G_{\text{subcooled melt}} = G_{\text{liquid}} \qquad\qquad \{2.15\}$$

$$G_{\text{activated state}} = \psi\, G_{\text{crystal}} + (1-\psi)\, G_{\text{liquid}} + 2b_0\sigma l \qquad\qquad \{2.16\}$$

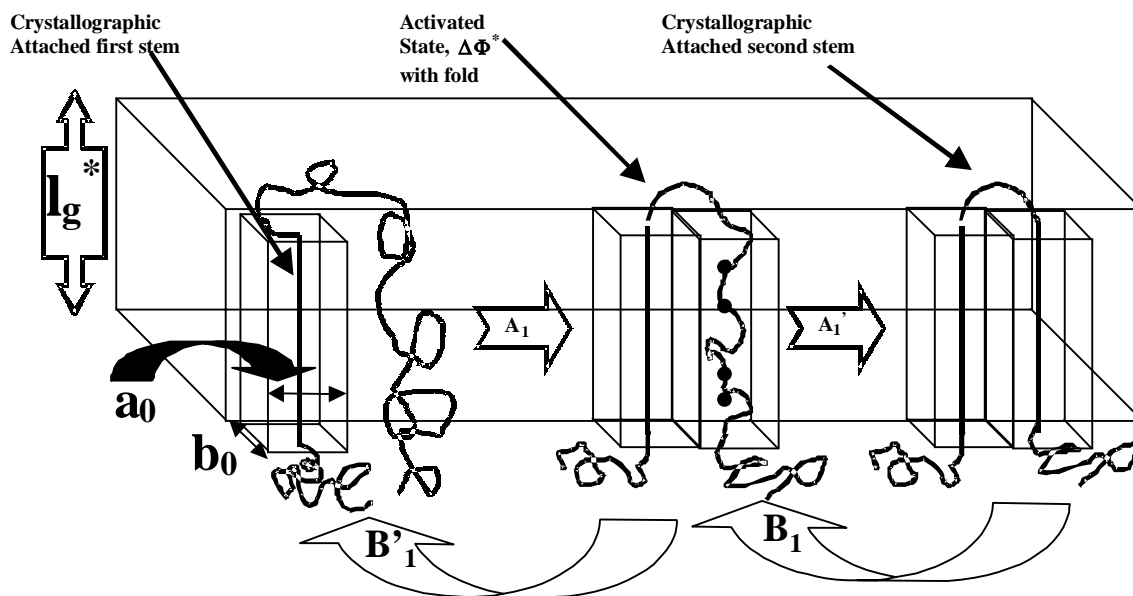$$G_{\text{attached stem}} = G_{\text{crystal}} + 2b_0\sigma l \qquad\qquad \{2.17\}$$

Also the change in free energy when going from subcooled melt to the activated stem is:

$$\Delta G_c^* = 2b_0\sigma l + \psi\,[a_0 b_0 l]\,\Delta G_c \qquad\qquad \{2.18\}$$

where ΔG_c is the free energy of crystallization/unit volume and 'ψ' is the apportionment factor, i.e. the fraction of free energy available due to the crystallographic attachment at a finite and few number of sites. The possible values of 'ψ' can thus be between 0 and 1. The second important formalism is the deposition of second and subsequent stems. The process for second stem deposition is similar in that it also involves an activated complex formation, although the activated stem differs with respect to the surface energy terms. The activated complex for second stem deposition does not lead to creation of any additional lateral surfaces but now consists of a 'single fold' and the 'aligned part of the molecule'. The surface energy and area associated with this tight fold are σ_e and $2a_0b_0$ respectively.
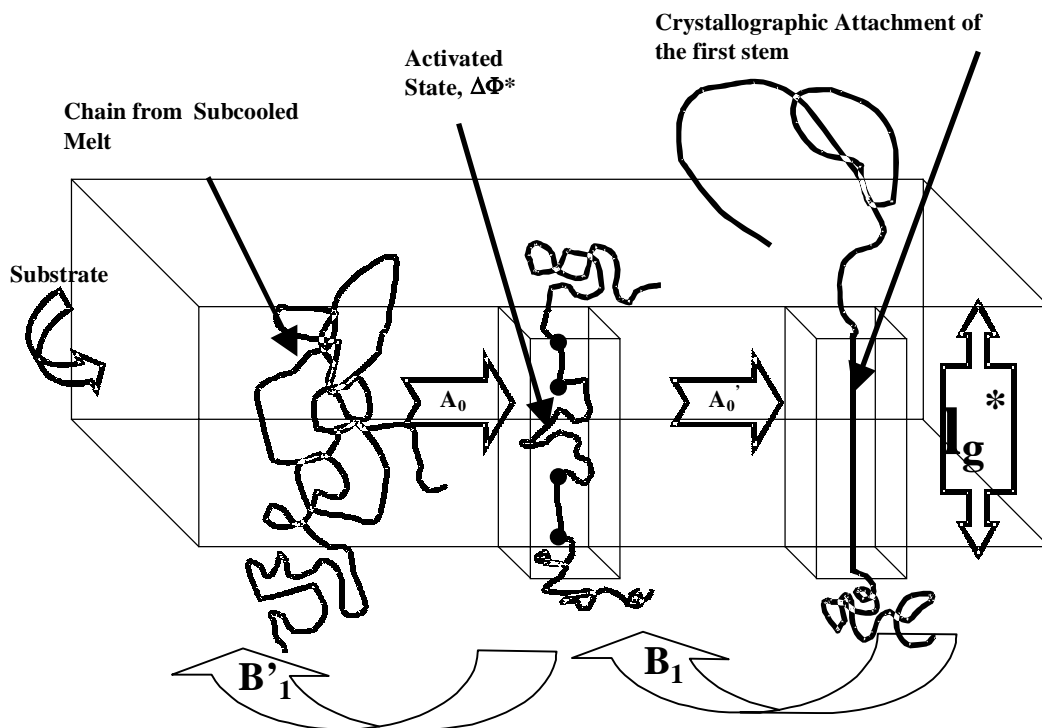
Figure 2.9   Formation of the physically aligned activated complex and its conversion to first crystallographically attached stem. The first step A_0 is the slowest and rate determining step while the step A_0' is fast[39].

Figure 2.10 Formation of the physically aligned activated complex and its conversion to second crystallographically attached stem. The first step A_0 is the slowest and rate determining step while the step $A_0^{'}$ is fast. The activated state includes a tight fold + the aligned part of the chain[39].

The free energy for the unattached part, in the various states is then:

$$G_{initial} = G_{liquid} \qquad \{2.19\}$$

$$G_{activated\ state} = \psi\ G_{crystal} + (1-\psi)\ G_{liquid} + 2a_0b_0\sigma_e \qquad \{2.20\}$$
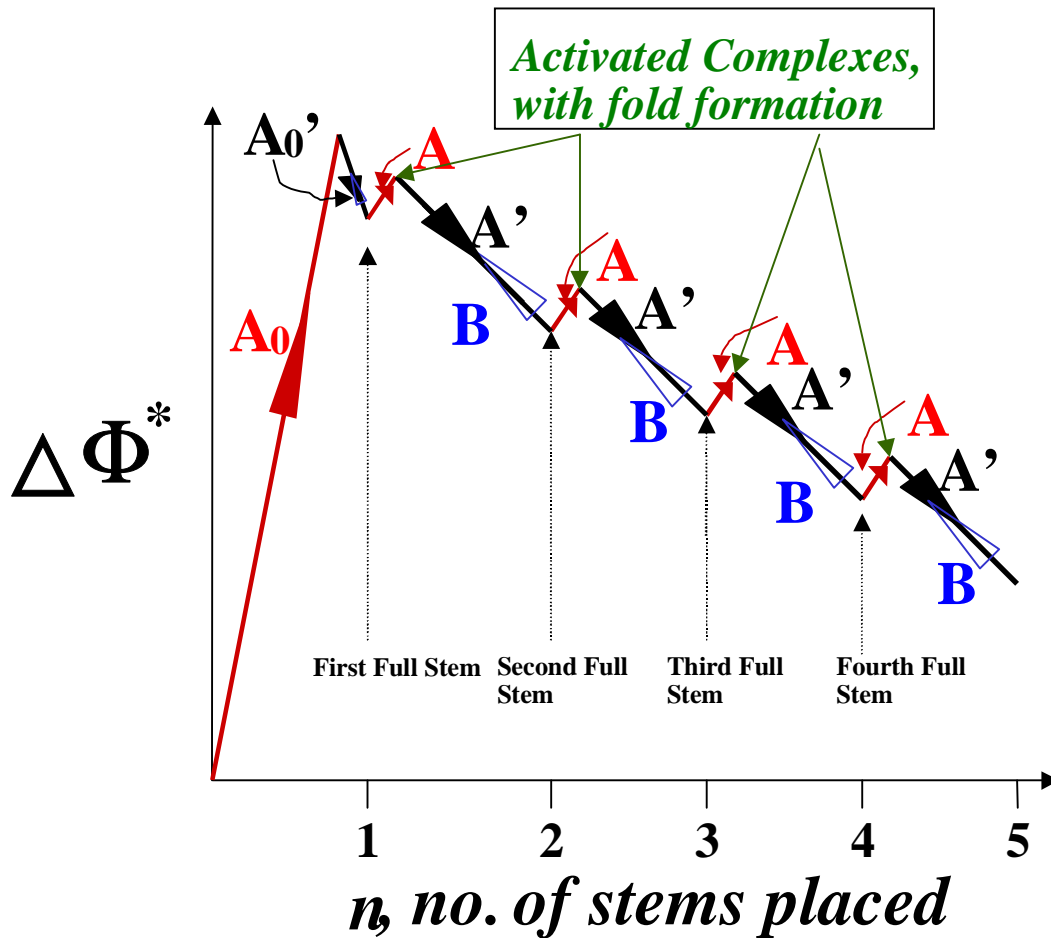
$$G_{attached\ stem} = G_{crystal} + 2a_0b_0\sigma_e \qquad \{2.21\}$$

Also the change in free energy when going from the subcooled melt to the activated state is:

$$\Delta G_c^* = 2a_0b_0\sigma_e + \psi\ [a_0b_0l]\ \Delta G_c \qquad \{2.22\}$$

For the nucleus to become stable, the slope of ΔG vs. ν curve should be negative. Thus:

$$2a_0b_0\sigma_e + [a_0b_0l]\ \Delta G_c < 0 \qquad \{2.23\}$$


Figure 2.11 Barrier system for the surface nucleation showing both the slow, fast and backward steps possible. A, A_0, B_1 and B are the rate determining slow steps while A_0' and A' are the fast steps[32].

$\Rightarrow l > 2\sigma_e/\Delta G_c$ for the nucleus to be stable

$$\Rightarrow l > \frac{2\sigma_e T_m}{\Delta H_f \Delta T_c} \qquad \{2.24\}$$

This means that $l_{min} = 2\sigma_e / [\Delta H_f \Delta T_c/T_m]$ is the *critical minimum length* needed to form a thermodynamically stable nucleus. This is schematically illustrated in Figure 2.11 which shows that the free energy actually rises as more and more stems are laid down, thus making the nucleation of those stems thermodynamically unfavorable. The figure also shows the length l_g^* at which the rate of stem deposition is kinetically favored, although it does not mean that the nucleus of such a length is thermodynamically most favored
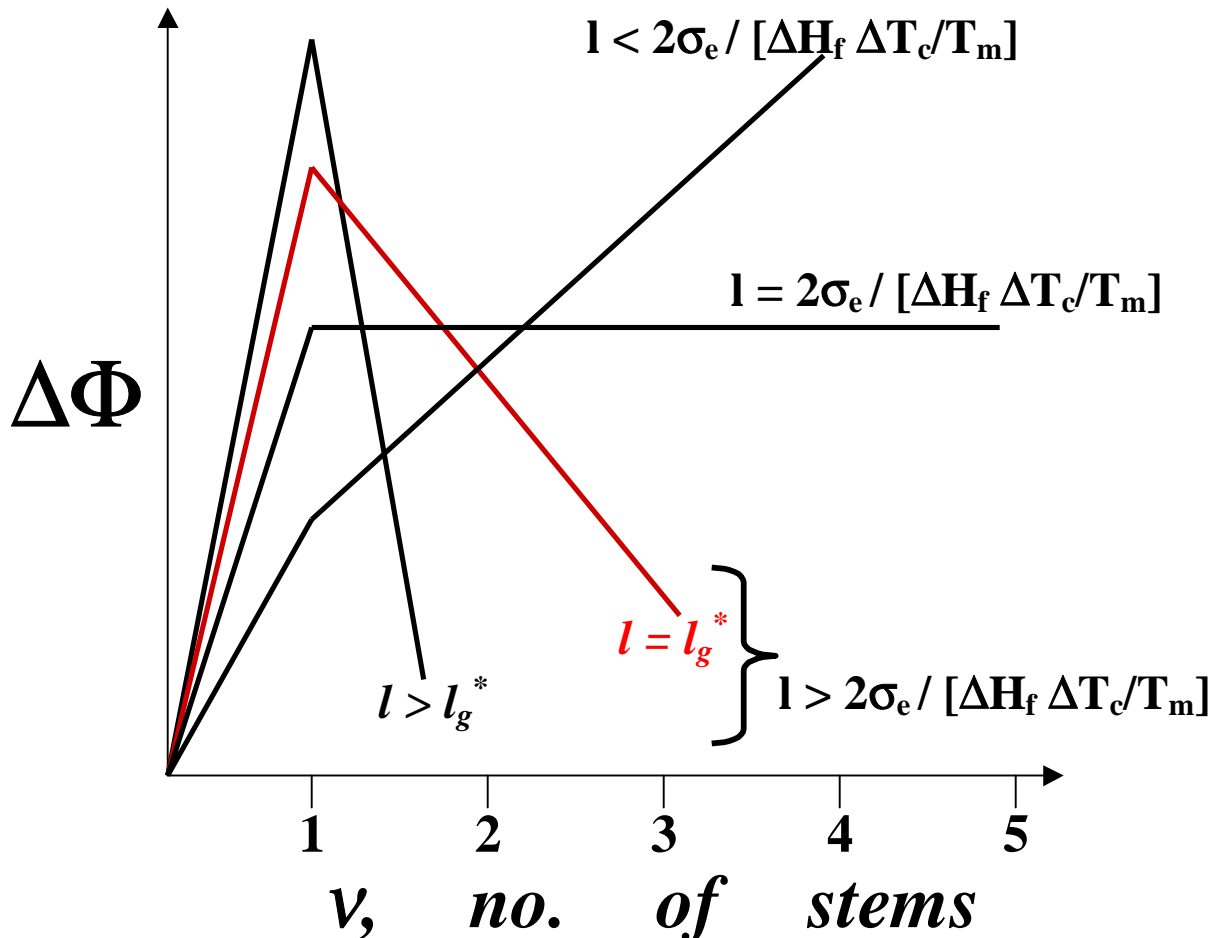
Figure 2.12 Free energy with subsequent stem deposition along the substrate for different values of lamellar thickness' 'l'[30].

(fully extended chain crystal will be such a case and not a chain folded one). *Thus the value of l which gives the fastest substrate completion rate and thus the maximum overall crystal growth rate 'G' (at that temperature) is the favored stem length for deposition, the average being l_g^*.* Subsequent flux calculations lead to an expression for l_g^*. It can be shown conveniently by steady state flux calculations that the rate of stem deposition is given by[49]:

$$S(l) = \frac{N_0 A_0 (A - B)}{A - B + B_1} \qquad \{2.25\}$$

Where N_0 is the number of initial stems, soon to be involved in the first stem deposition process. The values of the rates along various paths A_0, A, B_1 and B are estimated by Arrhenius rate expressions, the values of traditional activation energy in these being given by free energy barriers for the respective processes. Thus,

$$A_0 = \beta' \exp\left[\frac{-2b_0 l\sigma + \psi' a_0 b_0 l\Delta G_f}{kT_c}\right] \dots\dots\dots\dots\dots\dots\{2.26\}$$

$$B_1 = \beta' \exp\left[\frac{-(1-\psi') a_0 b_0 l\Delta G_f}{kT_c}\right] \dots\dots\dots\dots\dots\dots\{2.27\}$$

$$A = \beta \exp\left[\frac{-2b_0 l\sigma_e + \psi a_0 b_0 l\Delta G_f}{kT_c}\right] \dots\dots\dots\dots\dots\dots\{2.28\}$$

$$B = \beta \exp\left[\frac{-(1-\psi) a_0 b_0 l\Delta G_f}{kT_c}\right] \dots\dots\dots\dots\dots\dots\{2.29\}$$

The above expressions suggested by Marand *et al*[37,42,50,51] treat the pre-exponential factor (β') and 'apportionment factor' (ψ') for the rates associated with first stem deposition to be different than β and ψ for the second and subsequent stem deposition. However, the traditional L-H theory treats β=β' and ψ=ψ', in part due to the difficulty associated with finding an analytical solution for the secondary nucleation rate *i* if these factors are not held equal. While the procedure for using the above equations to give analytical rate expression for *i* (for two limiting cases) and the implication thereof is outlined by Snyder

et al[50,51] it is not difficult to visualize that the rationale of assigning different values for first and later stems is based on firmer grounds. While the short-range motions and localized conformational rearrangements (reptation of slack) are expected to govern the placement of the first stem, the later process is more akin to a reptation like motion of the rest of the chain, leading to subsequent stem depositions. In this regard, the molecular weight dependency of β and β' has been assumed to be different, with β' showing little or no dependence on molecular weight[50] and $\beta^{39,51,52} \propto n^{-1}$. For the traditional L-H treatment the value of β (=β') depends upon the value of the friction coefficient per chain repeat unit ζ^{39}. This monomeric friction coefficient ζ can itself be described by a Arrhenius kind of expression for temperatures greater than T_g+100K and by Vogel-Fulcher type expression for temperatures between T_g and T_g+100K. In these ways the traditional L-H treatment can account for molecular weight dependence and temperature dependence of crystal growth rate 'G' to a reasonable extent.

One problem with the traditional L-H theory has been that it forecasts a critical undercooling $\Delta T^* = 2\sigma T_m / \psi a_0 \Delta H_f$ where the value of l_g^* is predicted to show a relative upswing, a feature not confirmed experimentally for any polymer at any undercooling. Several approaches have been suggested to circumvent or alleviate this dilemma where the barrier to first stem deposition appears to become zero, this problem has been traditionally referred to as the "δl catastrophe"[43,53]. This problem is directly related to assignment of the value for ψ and has been circumvented by assigning ψ=0 in the traditional L-H theory. Recent modifications have also addressed this problem by stating that if the $\psi \leq 0.2$ the value falls close to absolute zero and is thus not expected to occur[39]. The low value of ψ has additionally been argued to be justifiable on the basis of a small number of niches expected for the first stem and thus close to nil contribution due to enthalpy of crystallization. Additionally, Marand *et al*[51] have suggested that the "δl catastrophe" is the mathematical artifact of assuming that ψ for the placement of the first stem and ψ for the placement of subsequent stems are same. Starting with the low ψ formulation in the L-H theory, the initial average lamellar thickness can be calculated as:

$$\langle l \rangle = l_g^* = \frac{\int\limits_{2\sigma_e/\Delta G}^{\infty} lS(l)dl}{\int\limits_{2\sigma_e/\Delta G}^{\infty} S(l)dl}$$

{2.30}

where the values of S(l) is given by equation (2.25) and the A, A_0, B_1 and B are given by expressions previously stated with the value of $\psi=\psi'=0$ and $\beta=\beta'$. With some effort, it can then be shown that[45]:

$$l_g^* = \frac{2\sigma_e}{\Delta G_f} + \left[\frac{kT}{2b_0\sigma}\right]\left[\frac{\Delta G_f + 4\sigma a_0}{\Delta G_f + 2\sigma a_0}\right] = l_{min} + \delta l$$

{2.31}

where the second term on the right-hand side represents 'δl', the increment above the minimum lamellar thickness which makes the crystal to enter the thermodynamically stable state at the fastest rate and prevents the anomaly $T_m = T_c$.

Another factor of importance is the thickening of lamellar crystals (1) during the traditional DSC heating scan, i.e. non-isothermal thickening, and also/or (2) when these originally grown crystals are sitting at some temperature (may or may not be T_c) i.e. non-isothermal thickening. These thickening processes occur for a large number of polymers although it has been advocated that a crystalline 'α_c' relaxation, which involves chain movement along the crystal, is a necessary condition for any thickening to occur in the lamellae[42,54]. Such thickening, when and if it occurs, will lead to lamellae of different thickness than what had initially formed, the thickening coefficient being defined as:

$$\gamma = l/l_g^*$$

{2.32}

the thickness of the lamellae at the time of the melting being l. For no thickening the value of γ will obviously be 1 and the value of melting point corresponds to the original lamellae grown at temperature T_c. Now, using the value for l_g^* from the equation (2.31) and incorporating any thickening effects by including equation (2.32) shown above, the previously described Gibbs-Thomson equation (2.14) yields the value of melting point as a function of undercooling ΔT_c.

$$T_m = T_m{}^\circ \left[1 - \left(\frac{\Delta T_c}{\gamma T_m{}^\circ} \right) \left(\frac{1}{1 + \dfrac{\delta l \Delta H_f \Delta T_c}{2\sigma_e T_m{}^\circ}} \right) \right] \qquad \{2.33\}$$

Now if it is assumed that $\delta l \Delta H_f \Delta T_c \ll 2\sigma_e T_m{}^\circ$, and that γ is constant then the equation transforms to the Hoffman-Weeks relation, widely used to determine the value of equilibrium melting point for various polymers.

$$T_m = T_m{}^{\circ hw} \left(1 - \frac{1}{\gamma^{hw}} \right) + \frac{T_c}{\gamma^{hw}} \qquad \{2.34\}$$

where $T_m{}^{ohw}$ and γ^{hw} are the respective value of equilibrium melting point and the thickening coefficient as determined by a Hoffman-Weeks plot. It is clear from the above equations that this method of estimating $T_m{}^\circ$, although providing an approximation, is incorrect on rigorous grounds due to two major assumptions mentioned above. Specifically let us address the use of this technique for the more rigid and aromatic based systems such as PEEK and some semicrystalline polyimides. These polymers have shown plenty of evidence for the existence of lamellar structures and exhibit other similarities in crystallization behavior with flexible chain polymers, thus inviting the assumption from many workers that many features of the L-H treatment can be reasonably applied. However, it is important to note that the main assumption of L-H model of an adjacent reentry is not observed for this rigid chain polymers. Also, for most of these polymers, the assumption of a constant thickening coefficient holds well. The problems arise however due to the first assumption of $\delta l \Delta H_f \Delta T_c \ll 2\sigma_e T_m{}^\circ$, which in effect pictures the contribution due to the δl term to be small in comparison to the overall lamellar thickness in contributing to the melting point. While this assumption holds better for flexible polymers like polyethylene, there is not much evidence to support this view for more rigid chain systems. Unlike polyethylene which consists of short repeating units and thus the δl increment can consist of several of these units, more rigid polymers display significantly longer repeat units. Thus for these polymers, even if the δl term

consists of one such additional unit, then the contribution of δl term in increasing lamellar thickness and hence the melting point cannot be ignored. The traditional objections for a Hoffman-Weeks analysis then become even more severe for polymers similar to ones utilized in the current project. Therefore such analysis can only serve as a coarse estimate in attaining the value of $T_m{}^{\circ}$. A recent work addresses in some detail the efficiency of this analysis for flexible chain polymers, given the degree of acceptable error[54].

2.8 Growth rate determination and regime kinetics

The above-discussed concepts lead us to calculations involving the lateral substrate completion rate, S_T as given by equation (2.35) below. The steady state flux S_T is

$$S_T = \frac{1}{l_u} \int\limits_{2\sigma_e/\Delta G}^{\infty} S(l)\,dl \qquad \{2.35\}$$

where l_u is the monomer length.

This allows us to calculate the rate of stem deposition 'i', i.e. the surface <u>nucleation</u> rate in terms of <u>stems s^{-1} cm^{-1}</u> by the simple relation[39]

$$i = S_T/L = S_T/n_l a_0 \qquad \{2.36\}$$

where n_l is the number of stems of width a_0 which make up the substrate of length L. The second important parameter leading up to the crystal growth rate 'G' is given by the substrate <u>completion</u> rate 'g'. The substrate completion rate is given by

$$g = a_0\,(A\text{-}B) \qquad \{2.37\}$$

Together the substrate nucleation rate 'i', and substrate completion rate 'g' decide the crystal growth rate 'G', the exact nature of this relation being given by relative rates of i vs. g. This issue and the relationship between i, g & G are illustrated in Figure 2.12.

Thus, three regimes of crystallization are considered in this problem. In Regime I[53,55], the growing crystal nucleus sweeps completely across the crystalline interface before any new nuclei are laid down. In Regime II[53,55], the relative rates of i vs. g are similar, thus allowing for the new nuclei to form even before the previous layer has completely been filled. In Regime III[56,57], a large amount of nucleation events occur and hence little or no substrate completion takes place. These three regimes have been experimentally observed for a large number of polymers and the undercooling dependencies of the growth rates in accordance with the above analysis has been confirmed (when using some adjustable fitting parameters).

Quantifying the analysis further, from the relations shown (Equations 2.35, 2.36 and 2.37 above and Equations 2.28, 2.29 and 2.31 shown previously) one obtains the substrate nucleation rate i and substrate completion rate g as[50]:

$$i = \frac{N_0 \beta}{n_l a_0 l_u} \left[\frac{kT}{2b_0\sigma} - \frac{kT}{2b_0\sigma + \Delta G_f} \right] \exp\left[\frac{-4b_0\sigma_e\sigma}{\Delta G_f kT} \right]$$

$$\{2.38\}$$

$$g = a_0 \beta \left[1 - \exp\left(\frac{a_0 b_0 \delta l \Delta G_f}{kT} \right) \right] \exp\left[\frac{-2a_0 b_0 \sigma_e}{kT} \right]$$
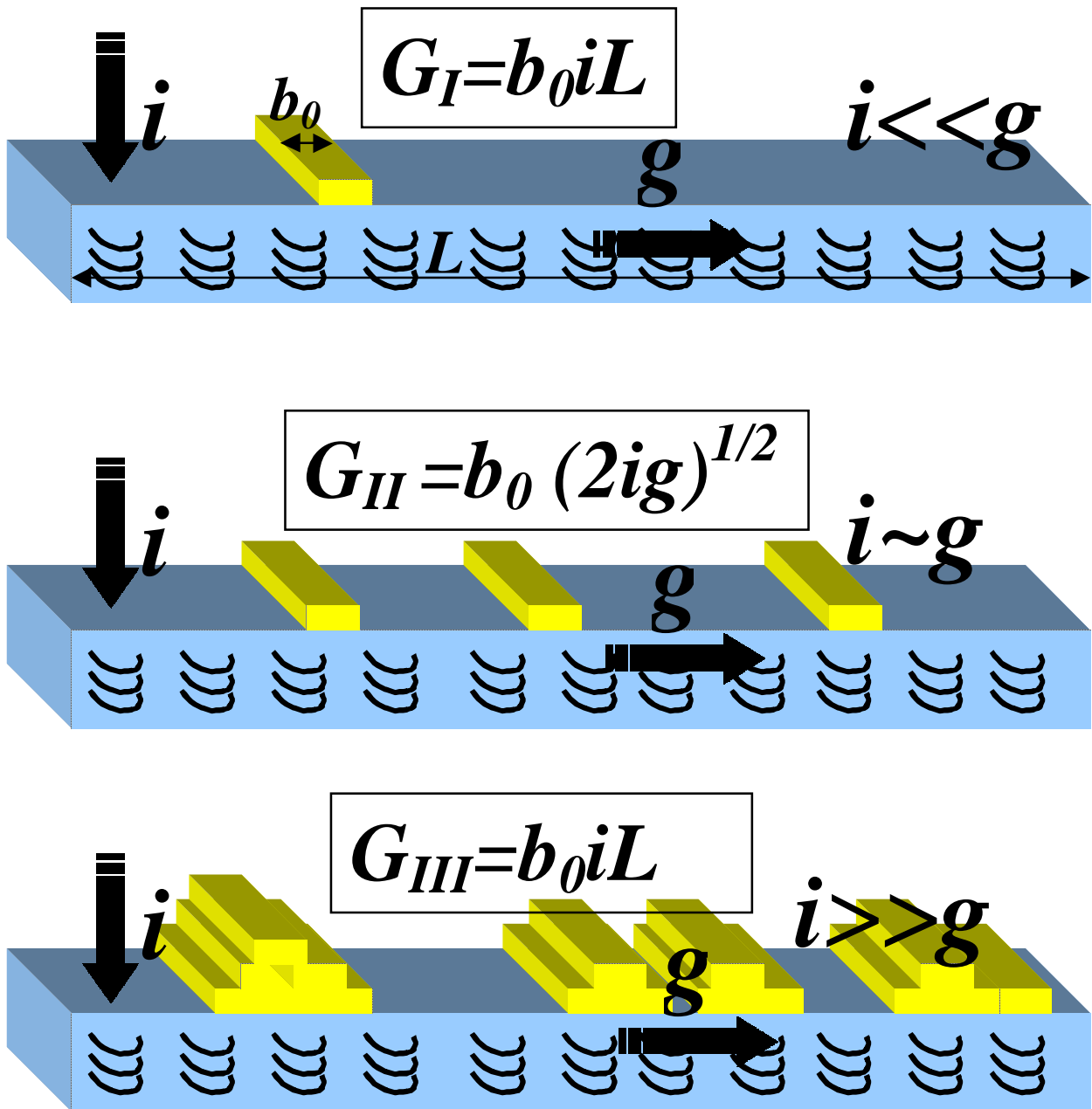
Figure 2.13 Scheme illustrating the rates of stem deposition during three different regimes of crystallization. 'i' represents the rate of stem nucleation whereas 'g' represents the rate of substrate completion.

As has been discussed before the parameter β in the above relations can be given by Vogel-Fulcher or Arrhenius type expressions. In the Arrhenius region, this factor can be described as:

$$\beta = J \exp\left[\frac{-U^*}{R(T-T_\infty)}\right] \qquad \{2.39a\}$$

where U^* is the activation energy and J is a factor with some degree of temperature dependence. In the recent version of the theory[39] it is given as:

$$J = \frac{\kappa}{n}\left(\frac{kT}{h}\right) \qquad \{2.39b\}$$

Here 'kT/h' is the frequency factor in events per second and 'n' is the number of repeat units. 'κ' is a numerical constant which is evaluated from the monomeric friction coefficient. These equations when substituted in the relations shown in the schematic give the crystal growth rate 'G' for the three different regimes as:

$$G_I = G_{0I} \exp(-U^*/R\ (T-T_\infty)) \exp(-K_{gI}/T\Delta T_c) \qquad \{2.40a\}$$

$$G_{II} = G_{0II} \exp(-U^*/R\ (T-T_\infty)) \exp(-K_{gII}/T\Delta T_c) \qquad \{2.40b\}$$

$$G_{III} = G_{0III} \exp(-U^*/R\ (T-T_\infty)) \exp(-K_{gIII}/T\Delta T_c) \qquad \{2.40c\}$$

Where,

$$G_{0i} = \frac{N_0 b_0 J}{l_u}\left[\frac{kT}{b_0\sigma} - \frac{kT}{2b_0\sigma + a_0 b_0\Delta G_f}\right] \qquad \{2.41\}$$

$$K_{gI} = K_{gII} = 2K_{gIII} = \frac{4\sigma\sigma_e T_m}{k\Delta H_f} \qquad \{2.42\}$$

The value of the nucleation constants K_{gI}, K_{gIII}, K_{gII} and G_{0i} can thus be determined by plotting the spherulitic growth rate data in the form $LnG + U^*/R\ (T-T_\infty)$ vs. $1/\ T\Delta T_c$. These types of plots are usually referred to as L-H plots and Figure 2.13 illustrates the typical plots for polymers showing these transitions. The first exponential term in equation (2.40), $\exp(-U^*/R\ (T-T_\infty))$ accounts for the chain transport effects to the interface while the second term $\exp(-K_{gi}/T\Delta T_c)$, accounts for the secondary nucleation effects. The widely utilized values for U^* and T_∞ are 1500 cal/mol and T_g-30K for a

large number of polymers[39,43]. L-H plots have also been widely utilized to obtain values for $\sigma\sigma_e$ if the values of $T_m{}^\circ$, ΔH_f and b_0 are known[40,58,59,60], or otherwise sometimes to obtain $T_m{}^\circ$ [54,61,62].
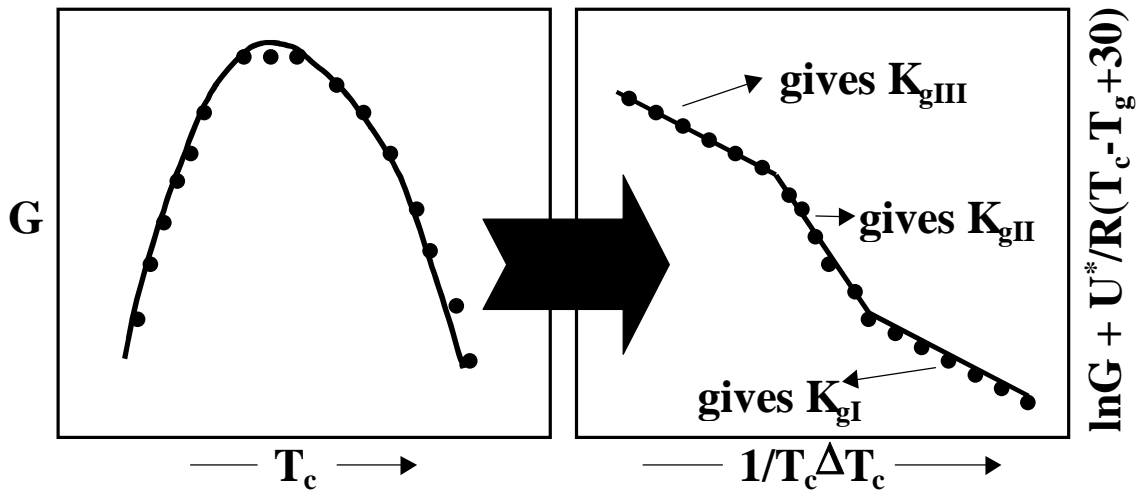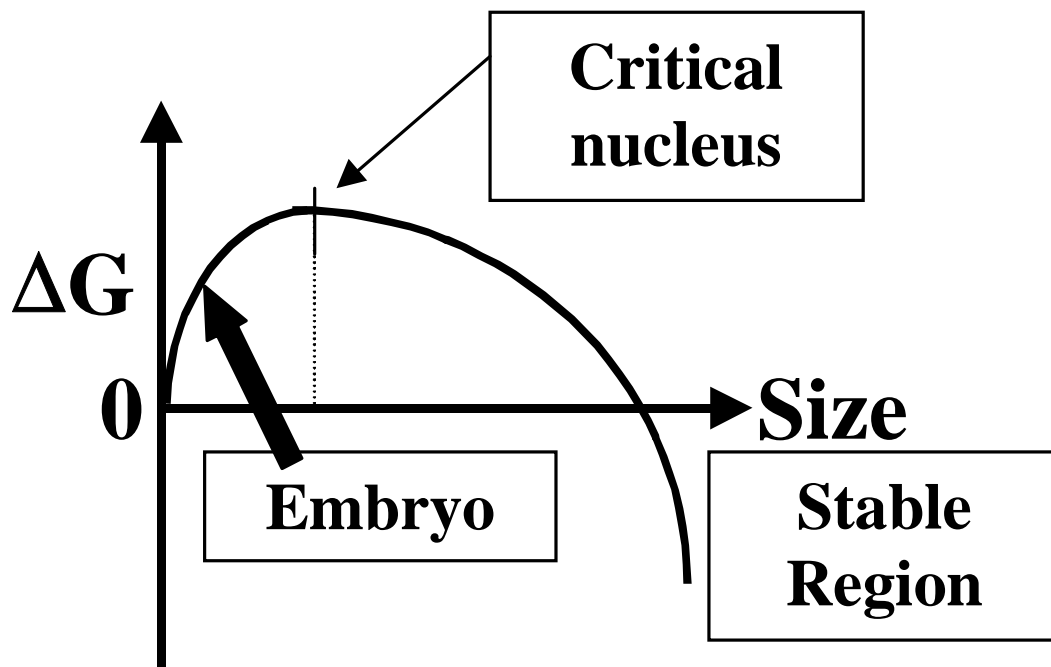

Figure 2.14 A schematic illustrating the conversion of growth rate data to a L-H plot showing the three regime transitions[38]. The values of regime constants are calculated by the slope in various regimes and are used to give the product of surface energy terms $\sigma\sigma_e$. All three regimes or even a single regime transition may not be experimentally observed for many polymers.
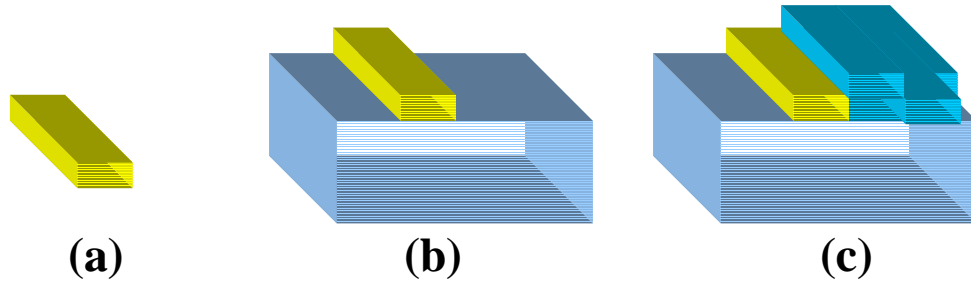
2.9 Primary nucleation:

For polymer crystallization to start, the primary nucleation first needs to take place. The nucleation itself can be defined as formation of a small amount of crystalline material due to fluctuations in density or order in the supercooled melt[63]. The formation of these initial or primary nuclei is the first step inaugurating crystallization and the phenomenon is called primary nucleation. The continuation of crystallization on the growth surface by induction of more and more polymer molecules is referred to as secondary nucleation and the previously discussed L-H theory addresses this issue. Another way of classifying nucleation is by invoking the prerequisite for the original site where the nucleation occurs. If no second surface or existing nuclei (i.e. any type of second phase) is present and the nuclei formation takes place spontaneously only due to supercooling the phenomenon is referred to as homogenous nucleation. However, if any second phase is required (it may be a foreign particle or surface from the same polymer nuclei/crystal), then the nucleation is termed heterogeneous nucleation. Wunderlich *et al.*[5] based on an earlier work[64] have further advocated the subdivision of this classification by incorporating the third category called *self-nucleation*. This nucleation is due to preexisting/residual nuclei that survived the initial melt conditions (or the dissolution conditions if it is solution crystallization). Later studies covered in this report will show results, which indicate that this s*elf-nucleation* is very important with respect to understanding the melt crystallization behavior of semicrystalline polyimides, the subject of this study. It should be clear that while primary nucleation can be either homogenous or heterogeneous, secondary nucleation by its very definition is heterogeneous in origin. Yet another way of categorizing primary nucleation is on the basis of time dependent effects at any temperature. If the nucleation is such that all nuclei start forming at approximately the same time then the nucleation is referred to as *athermal* nucleation. One aspect of such nucleation is that it leads to spherulites of roughly the same size during isothermal crystallization. If the nucleation on the other hand is such that new nuclei form throughout the crystallization at a particular temperature, and thus different spherulitic (crystal) sizes are obtained than the nucleation is referred to as *thermal*

nucleation. It thus may not be difficult to visualize that homogenous nucleation is often of the thermal type (the converse is not true) whereas the heterogeneous nucleation may be thermal or athermal. In the case of self-nucleation, the nucleation type has generally been observed as athermal although work in the present project has confirmed that this is not a necessary condition.

For the formation of stable nuclei to take place (primary or secondary), the free energy barrier to crystallization needs to be overcome. The size of this critical nucleus required obviously depends upon this free energy barrier, larger critical nuclei requiring longer times to form. The concept is very similar to one discussed in L-H theory previously and is illustrated in Figure 2.14.

Figure 2.15 Schematic illustrating the variation of free energy with nucleus size. The initial free energy barrier needs to be crossed for the nucleus to become stable[5].

Figure 2.16   Types of Crystal Nuclei (a) Primary nucleus (b) Secondary Nucleus
(c) Tertiary Nucleus

In any nucleation process, the free energy of the nucleation process (crystallization) is given by:

$$\Delta G = \Delta G_c + \sum \gamma^* A \qquad \{2.43\}$$

where the specific surface free energy is given by γ^*. Primary nucleation involves the largest specific area while the area is somewhat reduced for secondary nucleation on the surface. Tertiary nucleation, which can be defined as nucleation at an edge, involves yet lesser specific area. Thus, in terms of difficulty of the nucleation process, it goes as[5]:

Primary nucleation > Secondary Nucleation > Tertiary Nucleation.

The large specific area to volume ratio of such entities offsets the decrease in free energy that can be obtained by crystallizing the small volume element of the nucleus. The fundamentals of such a nucleation process can be investigated by performing free energy calculations on the incipient nucleus. In this regard, for the general case of a spherical nucleus of radius 'r', the free energy change can be expressed as:

$$\Delta G = 4/3 \pi r^3 \Delta G_c + 4\pi r^2 \gamma^* \qquad \{2.44\}$$

These two opposing contributions to the free energy lead to an initial rise in ΔG till a certain critical maximum in free energy surface is reached at 'r*', beyond which there is a

precipitous drop in the free energy leading to formation of a stable nucleus. The critical point is found out by differentiating the above equation w.r.t. 'r' and equating it with zero. The values for such critical points thus obtained are[2]:

$$r = r^* = \frac{2\sigma}{\Delta G_c} = \frac{2\sigma T_m{}^\circ}{\Delta H_f \Delta T_c} \qquad \{2.45\}$$

$$\Delta G = \Delta G^* = \frac{16\pi\sigma^3}{3\Delta G_c{}^2} = \frac{16\pi\sigma^3 T_m{}^{\circ 2}}{3\Delta H_f{}^2 \Delta T_c{}^2} \qquad \{2.46\}$$
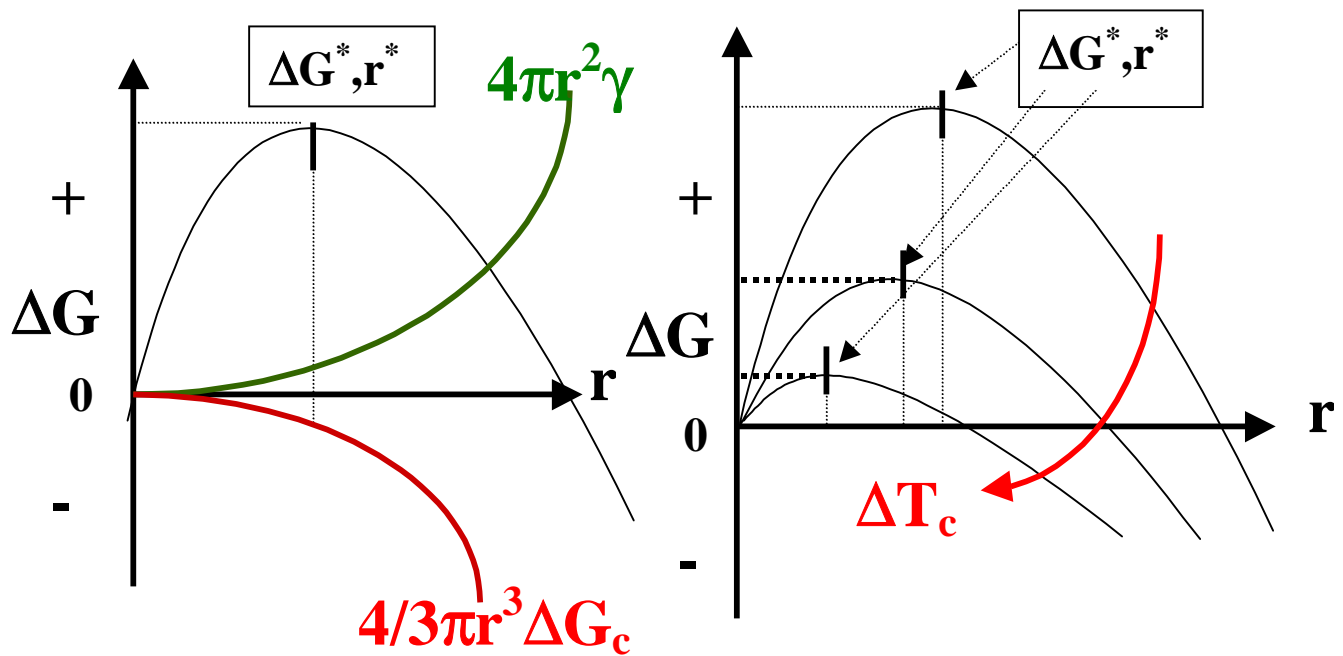
Figure 2.17 Variation of total free energy with size depends upon two opposing factors, the gain being due to increased surface area while the loss due to free energy of crystallization. Also, the critical size for stable nuclei formation as well as the critical free energy barrier decrease with increasing undercooling[2,38].

The critical size 'r*', and the critical free energy barrier are strongly dependent upon the undercooling ΔT_c. While $r^* \propto 1/\Delta T_c$, the free energy barrier $\Delta G^* \propto 1/\Delta T_c^2$. While the above analysis is for a spherical nuclei, the problems for other shapes such as cylindrical are more suited to polymeric nucleation and expressions for those can be similarly derived. It is very important to mention here that the shape of the nucleus will govern the final morphology of the crystallite, with the initial thickness of the crystallite being related to the critical size of the nucleus[2]. Turnbull and Fisher gave the steady state rate of nucleation per unit volume and time on the basis of transition state theory as[65]:

$$\dot{N} = N_0 \exp\left[-\frac{E_D + \Delta G^*}{RT}\right] \quad \{2.47\}$$

where $N_0 = n_1 kT/h$ is the number of molecules in a unit volume of the liquid. In this expression, ΔG^* is the activation energy derived above and E_D is akin to the free energy of activation for diffusion of chain segments to the phase boundary. The temperature dependence of the transport term E_D, is similar to that of viscosity with it remaining nearly constant at high temperatures and increasing rapidly at temperatures close to the glass transition. Till moderate undercoolings, the nucleation is dominated by the ΔG^* term which is $\propto 1/\Delta T_c^2$. Thus the nucleation rate is zero at T_m and has a large negative temperature coefficient just below T_m due to $\exp(-\Delta G^*/RT)$. At still larger undercoolings the influence of E_D term begins to increase and the nucleation rate reaches a maximum. At temperatures below the maximum, the nucleation rate is dominated by the transport term and has a large positive temperature coefficient with the rate falling to zero at temperatures below the glass transition. The above discussion can be applied with little modifications to heterogeneous nucleation with only the value of the constants varying[2]. The important geometry's of the heterogeneous type nucleation to which this type of analysis can be applied are fringed micelle and folded chain type nuclei. It is also important to recognize that various facets of the nucleation theory predict the experimentally observed features like, the negative temperature coefficient, and the variation of critical nucleus size (and hence the crystallite thickness) with undercooling. These predictions, however, are based on the most general premises, and thus do not

depend on the form, structure or chain disposition within the nucleus. The application of nucleation theory to the chain folded nucleus (L-H treatment), on its own, is thus not the proof of chain folded crystallization being prevalent[2,31,30].

2.10 Spherulites

The existence of these large (i.e. micron level) three dimensional supramolecular structures usually possessing three dimensional symmetry is a common occurrence not only in polymers but also in a large variety of inorganic substances and metals[66,67]. In fact, these kinds of structures have been found in rock specimens from the moon, which indicates that they grow during formation in rock strata[68]! In the case of polymers, these types of structures are conveniently observed in polarized optical microscope and consist of radial fibrils originating from a primary nucleus at the center. The large varieties of such structures that have been experimentally observed prohibit a strict definition though some general features can be summarized. The spherical shape arises usually due to small angle branching and splaying microstructure[69]. The initial stages of such a structure may not be spherical but rather may resemble a sheaf kind of morphology.
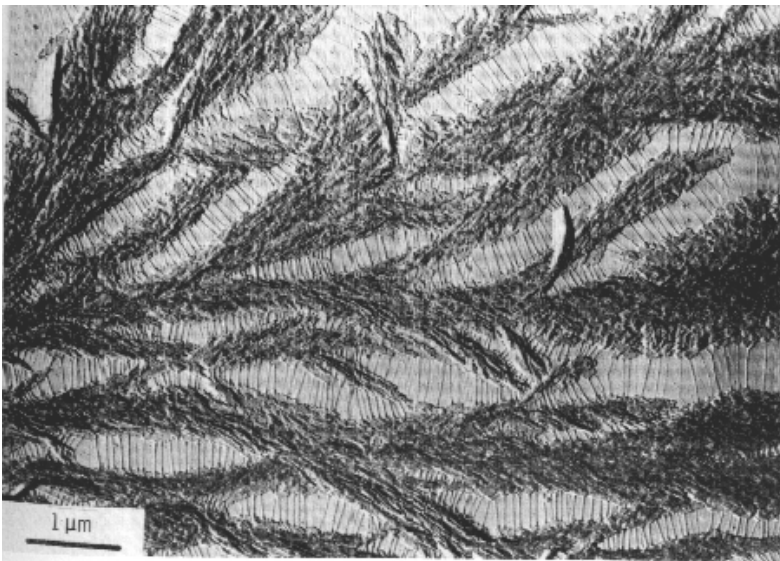
Figure 2.18 Tie chains in polyethylene spherulites crystallized in presence of n-parafin, $C_{32}H_{66}$, and then extracted with xylene at room temperature. (Keith and Padden[70] et al.)

Although the radial equivalency of this structure is usually a good approximation, this may not be true for the central core and also when the overall morphology becomes very coarse. The fibrils consist of lamellae radiating outward with the chain folding direction generally being transverse to the growth direction. Tie chains between these lamellae play an important role in improving the mechanical properties with these bridging units being both interlamellar and interspherulitic in origin. These links (Figure 2.17 from Keith and Padden[70]) help in maintaining the interlamellar connections when the polymer is drawn. On the basis of birefringence, the spherulites can be divided into the following categories[71]:

(a) Negatively birefringent: These are the most prevalent types of spherulites present in polymeric materials and are characterized by their refractive index along the transverse direction being greater than along the growth direction[72]. This optical character is due to the chain direction <u>on an average</u> being in transverse direction, this being a result of chain disposition within a lamella and lamellar arrangement within a spherulite.

(b) Positively Birefringent: These type of spherulites are observed when the refractive index along the radial direction exceeds that along the transverse direction. These types of spherulites are less common as the polarizability along the chain direction usually exceeds than along the other two principal directions. Such spherulites have been observed for polymers that have strong dipoles at large angle to the chain backbone and also exhibit chain tilt with respect to the growth direction.

(c) Zero birefringence: These type of spherulites are sometimes when the optic axis of the spherulites is aligned parallel to the viewing direction[73]. Random distribution of crystallites within the spherulite may also lead to such a structure.

(d) Chain-extended spherulites: These type have been observed during high pressure crystallization of polyethylene[74].

It has been traditionally believed[75] that smaller spherulitic sizes result in better impact strength and higher elongation to break. However, experimental studies supporting such conclusions continue to be scarce. Sharples[76] observed that the yield stress in Nylon 66 samples increased by 30% as the spherulitic size was decreased from 50 microns to 3 microns. Kargin *et al*[77]. demonstrated over a wide range of spherulitic sizes that the

mechanical properties deteriorated by 2-3 times whereas the elongation to break decreased from 500% to 25% as the spherulitic sizes were increased. Way *et al*[78]. showed that the yield stress of isotactic polypropylene goes through a maximum and then drops precipitously as the average spherulitic size was increased. This transition was concluded as being a result of deformation mechanism shifting from intraspherulitic yield to interspherulitic yield. Reinshagen[79] observed that isotactic polypropylene samples prepared under lower undercooling gave brittle interspherulitic fracture whereas samples prepared under larger undercoolings showed strain whitening and yielding before fracture.

2.11 Bulk crystallization kinetics-avrami analysis

Avrami Analysis[80,2,5] continues to remain the most popular method for obtaining bulk crystallization kinetics information. Its widespread use to obtain quantitative bulk crystallization kinetics knowledge is in part due to the relative ease with which the analysis can be applied. Unfortunately, this method has often been utilized without recognizing the assumptions and limitations of such an analysis, resulting in wrongful interpretations of experimental data. Before applying this analysis and correctly interpreting the data, it is important to understand the grounds on which this procedure was derived and the recognition of the assumptions that are involved. The mathematical foundation of this analysis is based on the famous raindrop problem first solved by Poisson[81] in 1837, which states that for raindrops falling randomly, the probability of a point being passed over by exactly F wavefronts is given by

$$P(F) = \frac{e^{-\overline{F}} \overline{F}^{F}}{F!} \qquad \{2.48\}$$

where $\overline{F}$ is the average number of such wavefronts passing through a point. Thus considering these wavefronts as spherulites in bulk crystallization, the probability of any point not being run over by a spherulite is given by value of P(F) at F=0. Thus

$$P(0) = e^{-\overline{F}} \qquad \{2.49\}$$

P(0) also represents the points which are still amorphous and not been run over by the spherulites and thus is equal to amorphous fraction 1-θ, where θ is the amount of fraction crystallized.

$$1 - \theta = P(0) = e^{-\overline{F}}$$

$$\Rightarrow \ln \frac{1}{1-\theta} = \overline{F} \qquad \{2.50\}$$

$$\Rightarrow \theta = 1 - \exp(-\overline{F})$$

Now the problem reduces to obtaining the form of the function $\overline{F}$ for different types of geometries that may be involved. The time dependency of the crystalline fraction in the above analysis enters due to time dependency of the function $\overline{F}$, the average number of wavefronts passing in time 't'. For some particular cases, this function can be calculated to give the following relations[5,82]:

(a) 2-dimensional case of growing discs starting at the same time

$$\overline{F} = \pi G^2 N t^2 \qquad \{2.51\}$$

where G is the growth rate of growing discs, N is the average number of such discs/area and t is the elapsed time.

(b) 2-dimensional case of growing discs forming at a rate $\dot{N}$

$$\overline{F} = \frac{\pi}{3} G^2 \dot{N} t^3 \qquad \{2.52\}$$

(c) 3-dimensional case of growing spheres starting at the same time

$$\overline{F} = \frac{4}{3} \pi G^3 N t^3 \qquad \{2.53\}$$

(d) 3-dimensional case of growing spheres forming at a rate $\dot{N}$

$$\overline{F} = \frac{\pi}{3} G^3 \dot{N} t^4 \qquad \{2.54\}$$

In general then, the form of the equation is of the type

$$\boxed{\theta = 1 - \exp(-K t^n)} \qquad \{2.55\}$$

which is the famous Avrami equation and the 'K' & 'n' are the two Avrami parameters usually referred to as the bulk crystallization constant (K) and Avrami exponent (n). As should be clear from the above analysis, 'K' is dependent on the *shape* of the growing crystalline entities and the *amount* and *type* of nucleation. The exponent 'n' is dependent
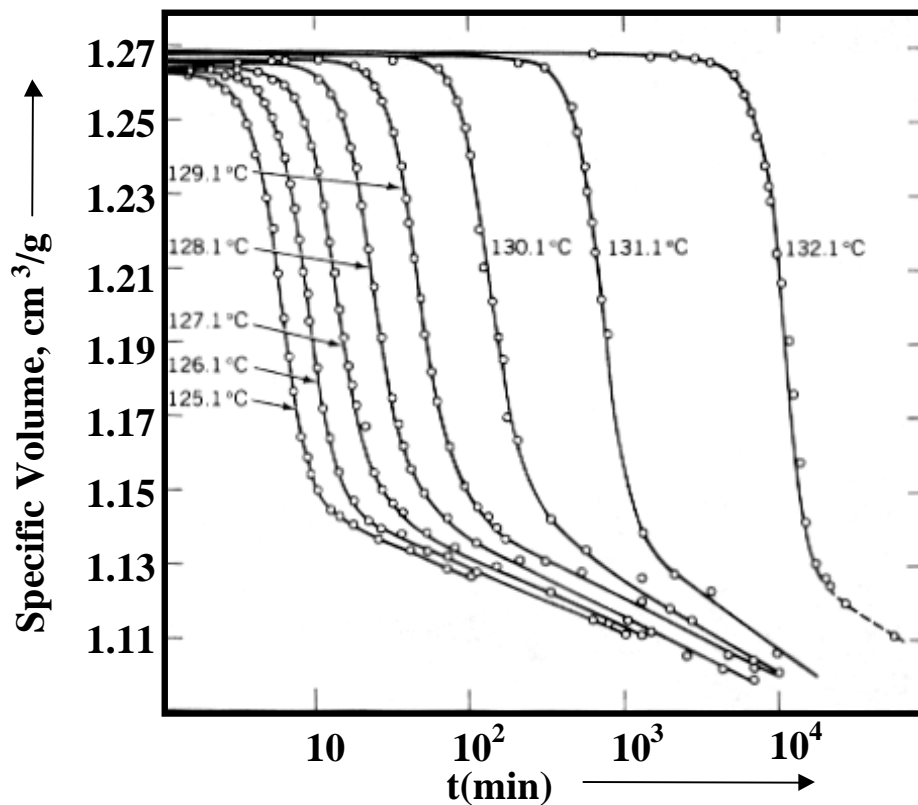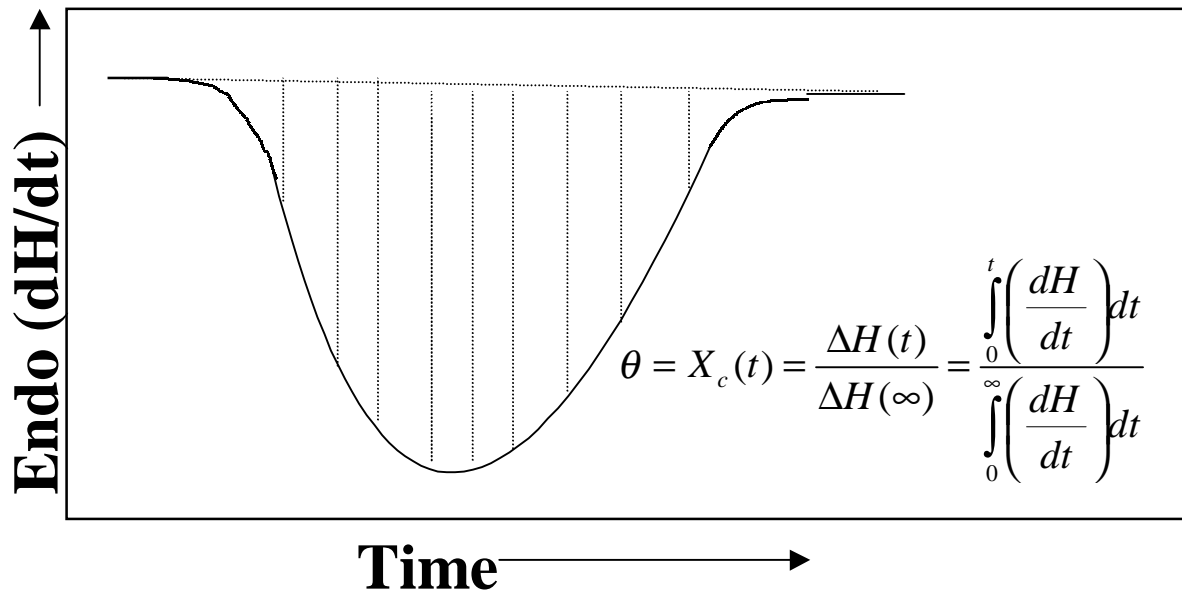
upon the nucleation *type* and growth *geometry* <u>but not on the amount of nucleation</u>. In the cases illustrated above it was tacitly assumed that the nucleation at the growth surface of the growing discs or spheres was the only governing factor in maintaining the growth rate G. In many instances, transport factors (like transport of heat of crystallization or transport of crystallizable molecules to the interface) become rate determining in controlling the rate of growth. These kind of problems involve a moving interface across which the transport phenomenon need to be considered and are usually referred to as Stefan problems[83] who applied it to study the thickness of polar ice caps. An example of this in polymers is the transcrystallization where nucleation is not the rate-determining factor. The solution to these kinds of problems is usually of the type[5,82]

$$G = \left[\frac{2\kappa}{t} \right]^{1/2} \qquad \{2.56\}$$

where κ is the diffusion constant. Thus the exponent of the time decreases by r$\times$0.5 for G^r present in the equation if the rate-determining step is transport/diffusion controlled. The various Avrami exponents associated with different nucleation types and crystal geometry's are shown in table 2.

Table 2.2.   Avrami exponents for various types of crystal growth geometry's[82].

Avrami Exponent	Crystal Geometry	Nucleation Type	Rate Determination
0.5	Rod	Athermal	Diffusion
1	Rod	Athermal	Nucleation
1.5	Rod	Thermal	Diffusion
2	Rod	Thermal	Nucleation
1	Disc	Athermal	Diffusion
2	Disc	Athermal	Nucleation
2	Disc	Thermal	Diffusion
3	Disc	Thermal	Nucleation
1.5	Sphere	Athermal	Diffusion
2.5	Sphere	Thermal	Diffusion
3	Sphere	Athermal	Nucleation
4	Sphere	Thermal	Nucleation

$$\theta = X_c(t) = \frac{\Delta H(t)}{\Delta H(\infty)} = \frac{\int\limits_{0}^{t}\left(\dfrac{dH}{dt}\right)dt}{\int\limits_{0}^{\infty}\left(\dfrac{dH}{dt}\right)dt}$$

Figure 2.19 Utilization of isothermal crystallization data by either DSC or by volume[30] measurements can give the degree of transformation, which can subsequently be utilized for Avrami analysis.
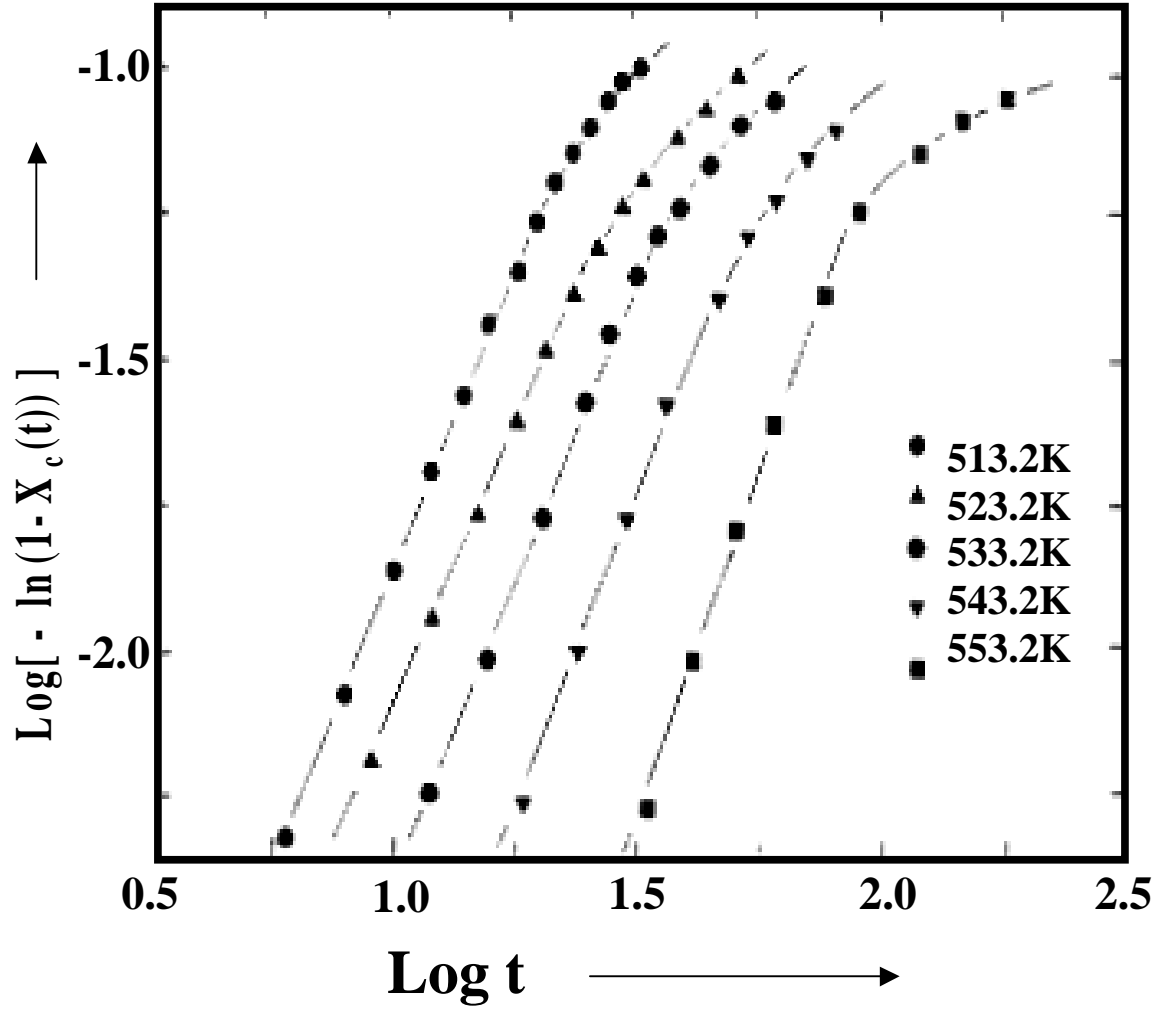
Figure 2.20 The characteristic Avrami plots obtained by isothermal crystallization experiments for a polyimide[84]. The initial slope of the curves gives the Avrami constant 'n', which is related to the crystal shape and nucleation type.

The traditionally utilized methods for measuring the crystalline fraction θ, have been the volume measurements and DSC in which the fraction θ is given respectively as:

Volume measurements: $\qquad \theta = \dfrac{V_t - V_0}{V_\infty - V_0}$ {2.57}

DSC measurements $\qquad \theta = \dfrac{\Delta H(t)}{\Delta H(\infty)}$ {2.58}

Where the V_t, V_0 and V_∞ represent the sample volume at time t, t=0 and at infinite time respectively. $\Delta H(t)$ and $\Delta H(\infty)$ represent the heat of crystallization obtained at time t and after infinite time. Figure 2.18(a) and Figure 2.18(b) illustrate the type of data obtained by the calorimetric and volumetric techniques and Figure 2.19[84] illustrates the conversion of such a data to give the characteristic Avrami plot. The Avrami equation (2.55) is analyzed by taking the double logarithm and writing in the form:

$$Log[-\ln(1-\theta)] = LogK + nLogt \qquad \{2.59\}$$

The crystalline fraction θ, is plotted in the form Log[-ln(1-θ)] vs. Log(t) to yield the characteristic Avrami plot. The initial slope of this plot (such as the one shown in Figure 2.19) gives the Avrami constant 'n'. The value of K is usually obtained by using the value of θ at t=$t_{1/2}$ and substituting in equation (2.56). With little effort, equation (2.56) yields:

$$K = \dfrac{\ln 2}{t_{1/2}{}^n} \qquad \{2.60\}$$

However before these techniques are utilized and interpretations regarding the crystallization kinetics made with the values of 'K' and 'n', it is important to recognize the inherent problems in Avrami analysis. The problems with the basic Avrami Analysis are[85,86,87,88]:

(a) The Avrami equation rigorously applies only to problems where the volume does not change. This is never the case with crystallization in polymers.

(b) It assumes constancy in the shape of growing disc/rod/sphere

(c) Constant radial growth is assumed ($G \sim t^{-1/2}$ has also been considered)

(d) The analysis does not account for the presence of an induction time

(e) The nucleation mode is assumed to be unique i.e. thermal or athermal but not both

(f) Complete crystallinity of the sample

(g) Random distribution of nuclei

(h) Constant value of radial density in the growing structures which is assumed in the derivation does not usually occur experimentally

(i) Holds well for primary crystallization only

(j) Does not account for absence of overlap between growing crystallization fronts

It is thus not surprising that non-integer values of n are often obtained. As shown in Table 2, it is not difficult to assign the experimentally obtained value of n by selecting an appropriate geometry. This kind of attribution of the exponent 'n', without independent microscopical evidence is one of the major pitfalls of most studies in the literature utilizing this analysis. *Independent microscopical evidence is critical before assignment of 'n' to a particular geometry can be justified.*

References:

[1] Cebe, P. and Hong, S.D., *Polymer*, 1986, **27**, 1183.

[2] Mandelkern, L. *Crystallization of Polymers*, McGraw-Hill, New York, 1964.

[3] Stejny, J., Dlugosz, J., and Keller A., *J. Mater. Sci*., pg. 1291, Vol. 14, 1977.

[4] Wegner, G., Organization of the Macromolecules in the condensed Phase, pg. 494, *Faraday Discussions of the Royal Society of Chemistry*, n68, 1979.

[5] Wunderlich, B., Macromolecular Physics, Vol. 2, Crystal Nucleation, Growth, Annealing, Academic Press, New York, 1976.

[6] Chanzy, H., quoted in *Treatise on Materials Science and Technology*, Vol. 10, Part A, Ed. Schultz, J.M., 1977.

[7] Pennings, A.J., "Crystal Growth", pg 389, Pergamon, Oxford, 1967.

[8] Pennings, A.J. and Kiel, A.M. *Kolloid Z.* 1965, **205**, 160

[9] Pennings, A.J. and Pijpers, M.F.J. *Macromolecules* 1970, **3**, 261.

[10] Keller, A., Organization of the Macromolecules in the condensed Phase, pg145, *Faraday Discussions of the Royal Society of Chemistry*, n68, 1979.

[11] Andrews, A.H., *Proceedings of the Royal Society (London),* A270, 232, 1962.

[12] Kobayashi, T. and Broutman, L.J., *Polym. Eng. Sci.* , 14, 260, 1974.

[13] Lindenmayer, P.H., *Molecular Composites: The future high performance plastics*. NSF August Rep., Washington D.C., 1974.

[14] McHugh, A.J., and Forest, E.H., *J. Macromol. Sci. Phys.* B11, 219, 1975.

[15] Herman, K., Gerngross, O. and Abitz, W. *Z. Phys. Chem.* 1930, **B10**, 371.

[16] Flory, P.J. *J. Chem. Phys.* 1949, **17**, 223.

[17] Flory, P.J. *J. Amer. Chem. Soc.* 1962, 84, 2857.

[18] Yoon, D.Y. and Flory, P.J. Organization of the Macromolecules in the condensed Phase, pg. 288, *Faraday Discussions of the Royal Society of Chemistry*, n68, 1979.

[19] Geil, P.H. in *Polymer Single Crystals*, 1963, John Wiley & Sons, New York, pg 9.

[20] Keller, A. *J. Polym. Sci.* 1955, **17**, 351.

[21] Girolamo, M., Keller, A., Miyasaka, K.K. and Overbergh, N. *J. Polym. Sci.* Part B, 1976, **14**, 39.

[22] Benson, R., Maxfield, J., Axelson, D.E. and Mandelkern, L. *J. Polym. Sci.* Part B, 1978, **19**, 1583.

[23] Storcks, K.H. *J. Am. Chem. Soc.* 1938, **60**, 1753.

[24] Schlesinger, W. and Leeper, H.M. *J. Polym. Sci.* 1953, **11**, 203.

[25] Jaccodine, R. *Nature* 1955, **176**, 305.

[26] Till, P.H. *J. Polym. Sci.* 1957, **24**, 301.

[27] Keller, A. *Phil. Mag.* 1957, **2**, 1171.

[28] Fischer, E.W. *Z. Naturforsch.* 1957, **12a**, 753.

[29] Flory, P.J. in *Structural Orders in Polymers* Ed. Ciardelli, F. and Gusti, P. 1981 Permagon Press, New York.

[30] Mandelkern, L. in *Characterization of Materials in Research: Ceramics and Polymers*, Syracuse Univ. Press, Syracuse, New York, 1975, pg. 369.

[31] Mandelkern, L., Organization of the Macromolecules in the condensed Phase, *Faraday Discussions of the Royal Society of Chemistry*, n68, 1979, 310.

[32] Hoffman, J.D. and Lauritzen, J.I., Jr. *J. Research NBS*, 1961, **65A**, 297.

[33] Hoffman, J.D. *SPE Transactions*, Oct 1964, 315.

[34] Fischer, E.W. *Pure Appl. Chem.* 1978, **50**, 1319.

[35] Fischer, E.W. Stamm, M., Dettenmair, M. and Herchenroder, P. *ACS Pol. Prepr.* 1979, **20**, 1, 219.

[36] Fischer, E.W. Stamm, M. and Dettenmair, M. Organization of the Macromolecules in the condensed Phase, *Faraday Discussions of the Royal Society of Chemistry*, n68, 1979, 263.

[37] Class Notes- "*Physical Chemistry of Polymers*", H. Marand, Virginia Tech, 1998.

[38] Class Notes- "*Polymer Morphology*", G.L. Wilkes, Virginia Tech, 1997.

[39] Hoffman, J.D. and Miller, R.L. *Polymer* 1997, **38**, 3151.

[40] Marand, H and Hoffman, J.D. *Macromolecules* 1990, **23**, 3682.

[41] Wunderlich, B., *Macromolecular Physics, Vol. 3, Crystal Melting*, Academic Press, New York, 1980.

[42] Marand, H., Xu, J. and Srinivas, S. *Macromolecules* 1998, *in print*.

[43] Hoffman, J.D., Davis, G.T. and Lauritzen, J.I. *Treatise on Solid State Chemistry*, Ed. Hannay, N.B., Plenum Press, New York, 1976, Vol. **3**, Chapter 7.

[44] Hoffman, J.D. and Miller, R.L. *Macromolecules* 1988, **21**, 3038.

[45] Hoffman, J.D. and Miller, R.L., Marand, H. and Roitman, D.B.. *Macromolecules* 1992, **25**, 2221.

[46] Hoffman, J.D., *Polymer* 1991, **32**, 2828.

[47] Mansfield, M.L. *J. Phys. Chem.* 1990, **94**, 6144.

[48] Lovinger, A.J. and Davis, D.D. *J. Appl. Phys.* 1985, **58**, 2843.

[49] Frank, F.C. and Tosi, M. *Proc. R. Soc. London, Ser A.,* 1961, **263**, 323.

[50] Snyder, C.R. and Marand, H. *Macromolecules* 1997 , **30**, 2759.

[51] Snyder, C.R., Mansfield, M.L. and Marand, H. *Macromolecules* 1996, **29**, 7508.

[52] DiMarzio, E.A., Guttman, C.M., Hoffman, J.D. Organization of the Macromolecules in the condensed Phase, *Faraday Discussions of the Royal Society of Chemistry*, n68, 1979, 210.

[53] Hoffman, J.D. and Lauritzen, J.I., Jr. *J. Appl. Phys.*, 1973, **44**, 4340.

[54] Xu, J., Srinivas, S. and Marand, H. *Macromolecules*, 1998, *in print*.

[55] Hoffman, J.D., Frolen, L.J., Ross, G.S. and Lauritzen, J.I., Jr. *J. Research NBS Sect. A* 1975, **79**, 671.

[56] Hoffman, J.D., Guttman, C.M. and Di Marzio, E.A. Organization of the Macromolecules in the condensed Phase, *Faraday Discussions of the Royal Society of Chemistry*, n68, 1979, 177.

[57] Hoffman, J.D., *Polymer* 1983, **24**, 3.

[58] Allen, R.C. and Mandelkern, L. *Polym. Bull.* 1987, **17**, 473.

[59] Fatou, J.G., Marco, C. and Mandelkern, L. *Polymer* 1990, **31**, 890.

[60] Heberer, D.P., Cheng, S.Z.D., Barley, J.S., Lien, S.H.S., Bryant, R.G. and Harris, F.W. *Maromolecules*, 1991, **24**, 1890.

[61] Huang, J. and Marand, H. *Macromolecules*, 1997, **30**, 1069.

[62] Huang, J., Prasad, A. and Marand, H. *Polymer*, 1994, **35**, 1896.

[63] Gibbs, J.W. in On the equilibrium of heterogeneous substances. *Trans. Conn. Acad.* **III**, 343. Also, "*The scientific works of J. Willard Gibbs*," Vol. **I**, 1906, Longmans, Green, New York, pg. 219

[64] Blundell, D.J., Keller, A. and Kovacs, A.J. *J. Polm. Sci. Part B*, 1966, **4**, 481.

[65] Turnbull, D. and Fisher, J.C. *J. Chem. Phys.* 1949, **17**, 71.

[66] Keith, H.D. and Padden, F.J., Jr. *J. Appl. Phys.* 1964, **35**, 1270.

[67] Marentette, J.M. and Brown, G.R. *J. Chem. Edu.* 1993, **70**, 435.

[68] Lofgren, G. *J. Geophys. Res.* 1971, **76**, 5635.

[69] Price, F.P. *J. Polym. Sci.* 1959 **37**, 71.

[70] Keith, H.D., Padden, F.J., Jr. and Vadimisky, R.G. *J. Polym. Sci. Part A-2* 1966, **4**, 267.

[71] Magill, J.H. in *Treatise on Materials Science and Technology* Ed. Schultz, J.M. 1977, **10**, 3.

[72] Keith, H.D. and Padden, F.J. *J. Polym. Sci.* 1959, **39**, 101.

[73] Magill, J.H. *J. Poly. Sci. Part A* 1966, **4**, 243.

[74] Basett, D.C. and Turner, B. *Phil. Mag.* 1974, **29**, 285.

[75] Lane, J.E. *Brit. Plast.* 1966, **39**, 528.

[76] Sharples, A. *Inroduction on Polymer Crystallization*, Arnold, London, 1966.

[77] Kargin, V.A., Sogolova, T.I. and Nadareishvilli, L.I. *Polym. Sci. USSR* 1964, **6**, 1404.

[78] Way, J.L., Atkinson, J.R. and Nutting, J. *J. Mater. Sci.* 1974, **9**, 293.

[79] Reinshagen, J.H. and Dunlap, R.W. *J. Appl. Polym. Sci.* 1975, **17**, 3619.

[80] Avrami, M. *J. Chem. Phys.* 1939, **7**, 1103.

[81] Poisson, S.D. "*Recherches sur la Probabilite des Jugements en matieres criminelle et en matiere civile*" Bachelier, Paris, pg. 206.

[82] Hiemenz, P.C. *Polymer Chemistry: The Basic Concepts* Marcel Dekker, New York, 1984, pg. 219.

[83] Stefan, J. *Ann. Phys. Chem.* 1891, **42**, 269.

[84] Heberer, D.P., Cheng, S.Z.D., Barley, J.S., Lien, S.H.S., Bryant, R.G. and Harris, F.W. *Macromolecules* 1991, **24**, 1890.

[85] Price, F.P. *J. Appl. Phys.* 1965, **36**, 3014.

[86] Grenier, D. and Homme, R.E.P. *J. Poly. Sci. Part B* 1980, **18**, 1655.

[87] Tomka, J. *Eur. Poly. J.* 1968, **4**, 237.

[88] Hillier, I.H. *J. Poly. Sci. Part A* 1965, **3**, 3067.